Fermi National Accelerator Laboratory

FERMILAB-Pub-94/204

Hadronic Radiotherapy

Arlene J. Lennox

Fermi National Accelerator Laboratory
P.O. Box 500, Batavia, Illinois 60510

Paula L. Petti

University of California
San Francisco, California 94143-0226

August 1994

Submitted to *Annual Review of Nuclear and Particle Science 1994.*

Operated by Universities Research Association Inc. under Contract No. DE-AC02-76CHO3000 with the United States Department of Energy

Disclaimer

HADRONIC RADIOTHERAPY

INTRODUCTION

Within a few months of Roentgen's discovery of X rays in 1895, investigators realized that X rays could be used for both diagnostic and therapeutic purposes. These soft X rays were far from optimal for radiation therapy, but new and better X-ray machines continually became available for clinical work as medicine took advantage of improved technology developed for basic science research. Today many hospitals and clinics use electron linear accelerators (linacs) with modern radiofrequency and controls systems to deliver 4- to 25-MeV electron beams, which can be used directly for therapy or targeted on tungsten to produce photons for therapy. Because of the low penetrating ability of electrons, electron therapy is used primarily to treat superficial diseases such as skin and lymph node tumors, whereas photon therapy has become the "workhorse" of radiation therapy.

Despite the advantages of modern electron linacs, extensive clinical experience with photon therapy has shown that some tumors, called radioresistant tumors, respond poorly to photon therapy, and that sometimes even nonradioresistant tumors cannot be given a tumoricidal dose because of the unavoidable associated dose to neighboring healthy tissue. Hadronic radiotherapy uses particles such as neutrons, protons, pions, helium, or heavier ions to treat radioresistant tumors and tumors located near critical body structures such as the spinal cord. Initial research in hadronic radiotherapy was performed using accelerators built for basic physics research. At present, there are a few hospital-based accelerators built for and dedicated to neutron and proton therapy, but much of the hadron therapy research continues to take place in physics laboratories. In this respect, the development of hadron therapy closely parallels the development of photon therapy. Advances in accelerator technology are making hadron therapy possible, although hadron therapy will not be as ubiquitous as photon therapy in the foreseeable future. This paper describes the physical and biological properties of different hadrons and their potential advantages for radiation therapy for various malignancies. Clinical results are presented along with examples of types of tumors for which hadronic radiotherapy has some proven benefit. We emphasize the essential contribution of technological advances in accelerator design and in diagnostic radiological techniques such as computed tomography (CT).

Physical Properties of Photons versus Charged Hadrons

In the therapeutic energy range (~0.1 - 25 MeV), photons interact with matter primarily via the Compton, photoelectric, and pair-production processes. Of these, the Compton process is the most important. Figure 1 shows depth-dose curves for photon beams of various energies. Within a distance of 0.5 cm - 3.0 cm in tissue, the dose "builds up" to a maximum and then falls off approximately exponentially in the patient. This so-called "build-up" region provides some degree of protection (often called "skin sparing") to the skin and subcutaneous layers. However, the dose at larger depths is significantly less than the maximum dose, and to treat deep-seated tumors effectively, one must use multiple (at least two) beams directed at the target from different angles so that the dose in the tumor is higher than the dose delivered near the surface and in surrounding healthy tissues. Figure 2 shows an example of a beam arrangement that might be used to treat a patient with a skull-base tumor. To give a uniform dose to the tumor while avoiding optic structures, three different beam directions are used.

The potential benefits of using protons and heavier charged particles for radiotherapy were first recognized by Wilson in 1946 (1). In the early 1950s, Tobias and his colleagues at the University of California Radiation Laboratory (UCRL) performed pioneering studies in animals that led to the use of protons and helium ions in treating human disease (2,3). In the therapeutic energy range (for protons, 70 - 250 MeV), charged particles lose energy primarily by ionizing and exciting electrons as they penetrate a medium. Because the energy deposited at a given depth is inversely proportional to the square of the particle's velocity, depth-dose curves for protons and heavier ions exhibit a sharp peak (called the Bragg peak) followed by a rapid decline in dose at the end of the particle range (Figure 3). Furthermore, although multiple scattering tends to degrade the Bragg peak in complex heterogeneous regions (4 - 7), the effects in homogeneous media are small. Clinically, the most important property of charged-particle beams is the sharp fall-off in dose at the end of the particle range. This sharp decrease is in direct contrast to the approximately exponential decrease in dose exhibited by photon beams and allows a higher tumor dose to be delivered without exceeding the tolerance dose of the surrounding normal structures.

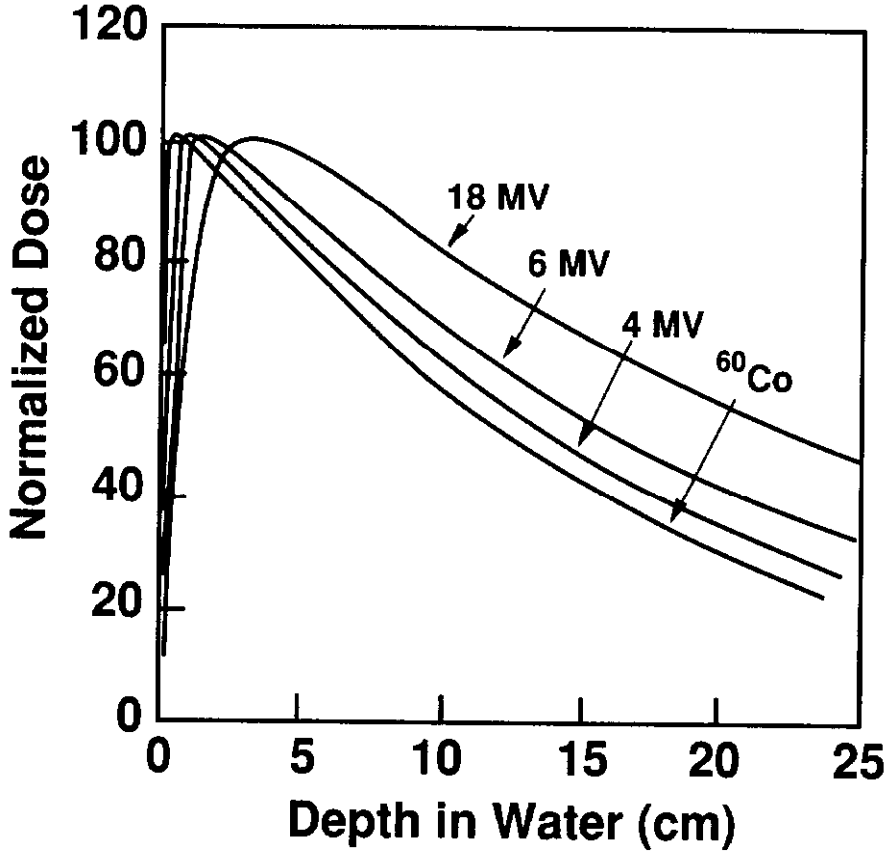

Figure 1: Sample depth-dose curves for photon beams used clinically in the treatment of cancer. With the exception of the ^{60}Co curve, these beams were produced by commercial linear accelerators. The energy designation on each of these curves corresponds to the energy of the electrons used to produce the bremsstrahlung photon beam. In radiation therapy, units of MV rather than MeV are used to describe beam energy.

Biological Properties of Photons versus Hadrons

In radiobiology, particle beams are often characterized by their linear-energy-transfer (LET) distribution. The LET of a particle is defined as the energy expended in creating ion pairs in the medium and is equal to the *restricted* stopping power. The difference between stopping power and restricted stopping power is that the former includes the energy spent in the production of delta rays, whereas the latter does not. LET is an important quantity because the amount of radiation damage incurred by a cell depends on the number of ionizing events produced by the radiation in the vicinity of the cell DNA. Radiation damage along a particle track is caused by both direct mechanisms in which DNA molecules are ionized by the particle and by indirect mechanisms in which free radicals produced by the ionizing particle react with the DNA. Because cells contain more than 70% water, most of the energy transferred by an ionizing particle goes into producing free radicals such as e^-_{aq}, ·OH and H·. Of these, ·OH generally is believed to be the most effective in causing radiation damage because it is an oxidizing agent and can extract a hydrogen atom from DNA (8).

The LET for 1-MeV electrons is 0.25 keV/μm. For neutrons produced in the reaction 50 MeV d + Be, the LET distribution ranges from 1.5 to 500 keV/μm, with peaks near 8 keV/μm and 100 keV/μm (9). Particles with LET values less than 30 - 50 keV/μm are called low-LET particles, whereas those with larger LET values are categorized as high-LET particles (10). High-LET particles are more biologically damaging because they cause more directly and indirectly ionizing events per unit track length.

The radiobiological rationale for high-LET radiotherapy is threefold (11): *(a)* Cells cannot repair the more extensive damage incurred by high-LET radiation as easily as they can repair low-LET radiation damage. *(b)* Tumor cells are often hypoxic, i.e. they lack oxygen because of an inadequate supply of blood

Figure 2: Dose distribution displayed on an axial CT slice for a patient with a skull-base tumor (meningioma). The dotted line represents the tumor, and the solid lines are isodose contours. The isodose lines are labeled to show the dose percentages relative to the maximum dose. Three beam directions are used: anterior-superior, right-anterior oblique, and left-posterior oblique.

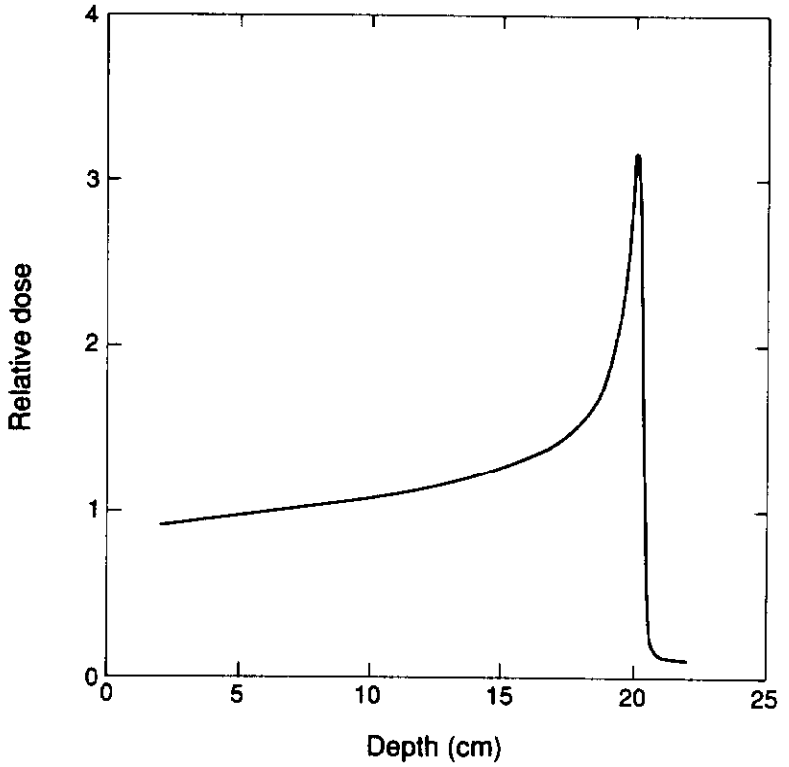

Figure 3: An example of a Bragg curve for a helium-ion beam used at LBL. The relative dose units are arbitrary.

to the tumor. Such cells are more responsive to high-LET than to low-LET radiation. This difference in response is due in part to the reduced production of oxidizing radicals under hypoxic conditions for low-LET radiation. *(c)* For low-LET radiation, cells exhibit varying degrees of radioresponsiveness depending on whether or not they are actively dividing. Certain cells are resistant to low-LET radiation when they are in the resting phase (i.e. G_1 or G_0) of the cell cycle (12). This radioresistance has clinical ramifications in terms of the types of tumors that might be most effectively treated with high-LET hadrons. It suggests that high-LET particles may be advantageous in treating slowly growing tumors with a significant fraction of cells in the G_1 and G_0 phases.

Radiobiologists use various quantities to describe the radioresponsiveness of cells. The oxygen-enhancement ratio (OER) is defined as the ratio of the dose required to achieve a given biological effect under hypoxic conditions to the dose required to achieve the same effect under oxygenated conditions. The OER for high-LET radiation is typically between 1 and 2, and the OER for low-LET radiation is between 2 and 3. Another way to characterize a given type of radiation is by its relative biological effectiveness (RBE). This quantity is defined as the ratio of the dose required to achieve a defined biological endpoint using some radiation standard to the dose required to achieve the same endpoint using the test radiation. Relative to ^{60}Co, the RBE for therapeutic neutron beams ranges from 3.0 to 3.3. For 160-MeV proton beams, the RBE is ~1.1, and for heavier particles, RBE values range from 1.2 to 4.5. In radiotherapy, the total dose is usually delivered over the course of several weeks. The amount of dose delivered in each treatment is called the fraction size. The RBE for hadron therapy depends on the fraction size as well as on the type of tissue irradiated and the position on the depth-dose curve at which the RBE is measured. Successful implementation of high-LET radiotherapy requires an understanding of the complicated dependency of RBE on these many variables.

Clinical Terminology

To assess the value of new or existing treatment modalities in cancer therapy, physicians often evaluate patients in terms of *local-control* rates or *survival* rates. A disease is considered locally controlled if there is no evidence of residual tumor in the irradiated volume as determined by a series of clinical and radiographic exams administered over the course of several years following treatment. Survival rates are evaluated differently by different investigators but usually include only deaths resulting from persistent

disease or treatment complications. Survival rates for a given disease and treatment modality generally tend to be lower than local-control rates because both treatment complications and the possibility that the tumor metastasizes affect survival, whereas local-control is not influenced by these factors.

FAST-NEUTRON THERAPY

Neutron therapy was the first form of hadron therapy to be used clinically. The rationale for fast-neutron therapy is biological, i.e. to take advantage of the high-LET distribution to control radioresistant tumors. When it was introduced, therapeutic neutron dosimetry was not well understood, and the variations in RBE with fractionation were not recognized. This lack of information ultimately caused early researchers to become discouraged about using neutrons for cancer therapy. Stone made the first attempts to use neutrons to treat advanced and otherwise untreatable tumors between 1938 and 1943 at UCRL, where 250 patients were treated (13). Early results were encouraging (14), but within a few years after treatment unacceptable skin damage occurred in many cases. In 1948, Stone concluded that neutrons had no place in cancer treatment because the side effects he observed far outweighed the clinical benefits (15). Researchers at Hammersmith Hospital reopened the whole question was in 1959 (16). After careful studies of the effects of neutron irradiation on the skin of pigs they concluded that Stone had severely overdosed the early patients (17). New clinical studies were begun in 1966 (18), and their encouraging results led to the development of neutron therapy clinical trials throughout the world. By 1980, 19 institutions had treated a total of nearly 6000 patients (19). In prescribing doses, physicians were guided by results of their own radiobiological experiments to determine RBE as well as better dosimetry protocols, and the overdoses that occurred in Stone's work were avoided.

Nevertheless, the large variation in beam characteristics at the different institutions hampered an accurate assessment of the clinical efficacy of neutrons. At first, all of the treatment centers used accelerators or neutron sources that had been built for other purposes. Each center used a beam with a unique energy spectrum, and the penetrating ability of many of these beams is now known to be unacceptable. As the problems caused by low energy beams were recognized, these centers either confined therapy to superficial disease or stopped clinical trials entirely. In the remainder of this paper the term "fast neutrons" refers only to beams produced by protons or deuterons with energy >48 MeV striking a beryllium target. Clinical trials using beams in this energy range began in the mid-1970s, and now, two decades later, it is becoming clear that although both the lower- and higher-energy beams control tumors, only the higher-energy beams do so without unacceptable long-term side effects.

Treatment Planning for Neutron Therapy

Fast-neutron beams have depth-dose characteristics similar to those of photon beams, including the skin-sparing effect illustrated in Figure 1, and treatment plans for fast neutrons are similar to photon treatment plans. A neutron beam generated by 66-MeV protons impinging on a beryllium target thick enough to dissipate 40 MeV exhibits a depth-dose curve similar to that produced by 8-MeV electrons striking a tungsten target to produce photons (20). Such a beam penetrates tissue well enough to treat deep-seated tumors. Energy deposition is not affected significantly by the presence of tissue heterogeneities, so dose calculations do not require the use of CT data. However, CT scans are used routinely to assist the physician in outlining the tumor and critical structures when planning the patient treatment.

Clinical Trials for Neutron Therapy

Fast neutrons are considered the treatment of choice for inoperable salivary gland tumors (21, 22), and they are also demonstrating an advantage in long-term survival for advanced prostate cancer. Figure 4 shows results of a 10-year study that compared treatment with photons only or with a combination of photons and neutrons (23). A later study with a median follow-up of 4.2 years compared treatment with photons only with treatment with neutrons only. This study also found fast-neutron therapy to be superior to photon therapy for local and regional treatment of advanced prostate cancer (24). Neutrons also are advantageous in treating selected patients with inoperable squamous-cell lung cancer (25).

Relatively few patients have been treated for soft-tissue sarcoma and osteosarcoma with neutrons, and to group them into meaningful categories for statistical analysis is difficult because in many cases the disease has already metastasized to different parts of the body. For these patients, neutron therapy effectively controls the local tumor and relieves local symptoms but does not necessarily prolong life. Nevertheless, local-control rates for neutron irradiation of bone and soft-tissue sarcoma are reportedly ~50% as compared

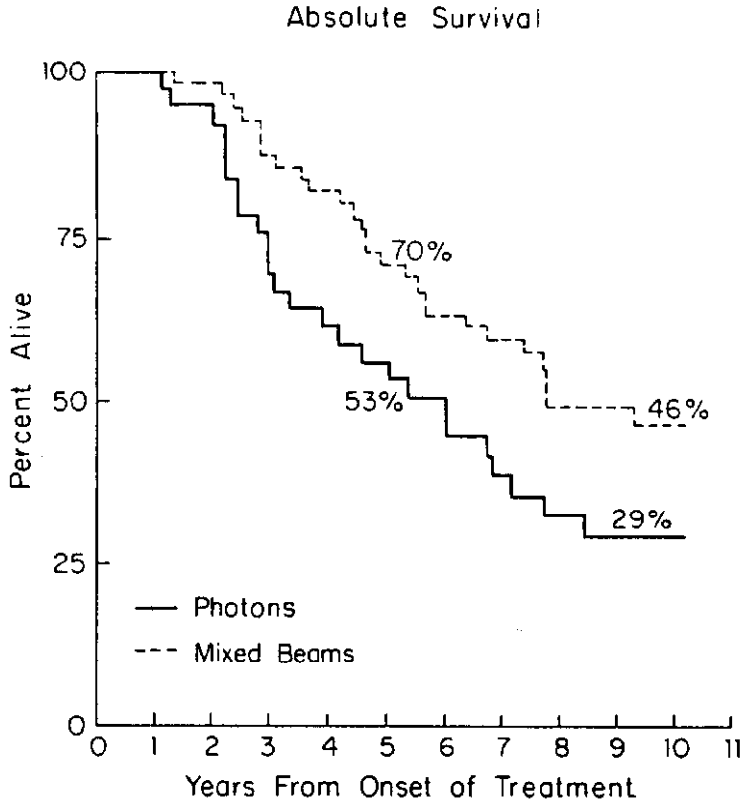

Figure 4: Survival curves for locally-advanced prostate cancer treated with photons only or with a combination of photons and neutrons. Redrawn from reference 23.

to between 20-30% for conventional photon or electron therapy (26). Fast-neutron therapy has also been used to treat advanced brain tumors (gliomas). However, these clinical trials were ended when investigators established that long-term survival was the same for neutron therapy as for photon therapy (27). At present, interest is focused on the use of boron-10 with fast neutrons to boost the tumor dose relative to the normal-tissue dose. The rationale for this approach is detailed in the section on neutron-capture therapy.

Treatment Centers and Accelerators for Neutron Therapy

Fast-neutron therapy is no longer considered to be experimental. It is reimbursed by insurance carriers, and a treatment center can be supported by operating on a fee-for-service basis. Clinics currently treating an average of about ten patients per day are located at Fermi National Accelerator Laboratory in Batavia, Illinois; the University of Washington in Seattle, Washington; Harper Grace Hospital in Detroit, Michigan; and the National Accelerator Centre in Faure, South Africa. Each of these treatment centers can position patients isocentrically and collimate the beam to match the tumor shape. Moreover, their dose rate is adequate and their accelerators reliable enough for clinical work. These technological capabilities have enabled clinicians to assess the effects of small differences in treatment protocols. For example, one study of treatments for advanced prostate cancer showed that lowering the prescribed dose from 21.0 to 20.4 Gy significantly reduced the probability of severe long-term side effects without compromising the probability of long-term local control (L Cohen, KR Saroja, FR Hendrickson, AJ Lennox, paper in preparation).

Both cyclotrons and proton linacs are used to accelerate protons or deuterons that strike a beryllium target to produce fast neutrons. Cyclotrons were developed before linacs, so much of the early work with neutron therapy was performed with cyclotrons. A notable exception was the use of 66-MeV protons from the Fermilab proton linac. Recent advances in the technology of radiofrequency quadrupole linacs and the use of 425-MHz drift tube linacs have made it possible to build hospital-based linacs with intensities sufficient to provide protons for fast-neutron therapy and isotope production while serving as an injector for a proton synchrotron for proton therapy (28). Because the building and operating costs for proton linacs have decreased to near those of cyclotrons, linacs are now being considered in the design of new hadron therapy centers.

LOW-LET CHARGED PARTICLES

Protons and helium ions are predominantly low-LET particles, and any therapeutic advantage they may have is a result of their physical properties. To fully exploit the sharp fall-off in dose following the Bragg peak, one needs an accurate three-dimensional description of the tumor in relation to critical organs in the patient. CT provides this detailed anatomical information. Tissue-density data, which are critical to charged-particle treatment planning, may also be inferred from CT, as discussed below.

Compensator Design and the Use of CT Data

Charged particles lose energy as they traverse a medium according to Bethe's formula (29):

$$\frac{dE}{dx} = \frac{2\pi z^2 e^4}{mc^2\beta^2}\rho_e\left[ln\frac{2mc^2\beta^2 W}{I_{adj}^2(1-\beta^2)} - 2\beta^2 - S - \Delta\right] \qquad (1)$$

where, $\frac{dE}{dx}$ is the energy loss per unit distance; ρ_e is the electron density of the material; z is the effective charge of the proton; e is the electronic charge in esu; $m\,c^2$ is the rest energy of the electron; I_{adj} is the adjusted ionization potential of the material; β is the ratio of the incident particle velocity to the velocity of light; W is the maximum kinetic energy that can be transferred to an electron initially at rest; S is a term describing shell corrections; and Δ is the polarization effect correction term.

The polarization effect term Δ is negligible for the particle energies used therapeutically. In human tissue, shell corrections are important only for protons or helium ions of very low energy. Differences in the logarithm of the ionization potential for different types of human tissue result in only small changes in the stopping power. Thus, for a given charged-particle beam whose energy is in the therapeutic range, dE/dx is roughly proportional to the electron density ρ_e of the material. The electron density at each point in a patient may be inferred from CT data that provide a measure of the linear-attenuation coefficients for the diagnostic X rays produced by the scanner. These linear-attenuation coefficients are proportional to the electron density of the material at each location. The average electron density along a given particle trajectory of length t in the patient is:

$$\rho_e^{ave} = \frac{1}{t}\int_0^t \rho_e(x)dx. \qquad (2)$$

The quantity, $t\rho_e^{ave} / \rho_e^{H2O}$, is defined as the water-equivalent pathlength along the trajectory and represents the thickness of water that produces the same energy loss as the actual thickness t in the patient. In practice, CT units must be calibrated by scanning materials with different electron densities and then measuring the water-equivalent range of the charged-particle beam in these materials (30 - 32).

One of the most important uses of CT data is the design of tissue compensators or boluses that control the beam penetration so that the distal surface of the dose distribution conforms to the distal surface of the target volume for each beam orientation (Figure 5) (33, 34). These devices are usually fabricated from wax or Lucite. To design a compensator, the water-equivalent distance along the beam trajectory to each point on the distal surface of the target volume is determined from the CT data. The thickness of the compensator at each of these points is then calculated by subtracting this water-equivalent distance from the beam range.

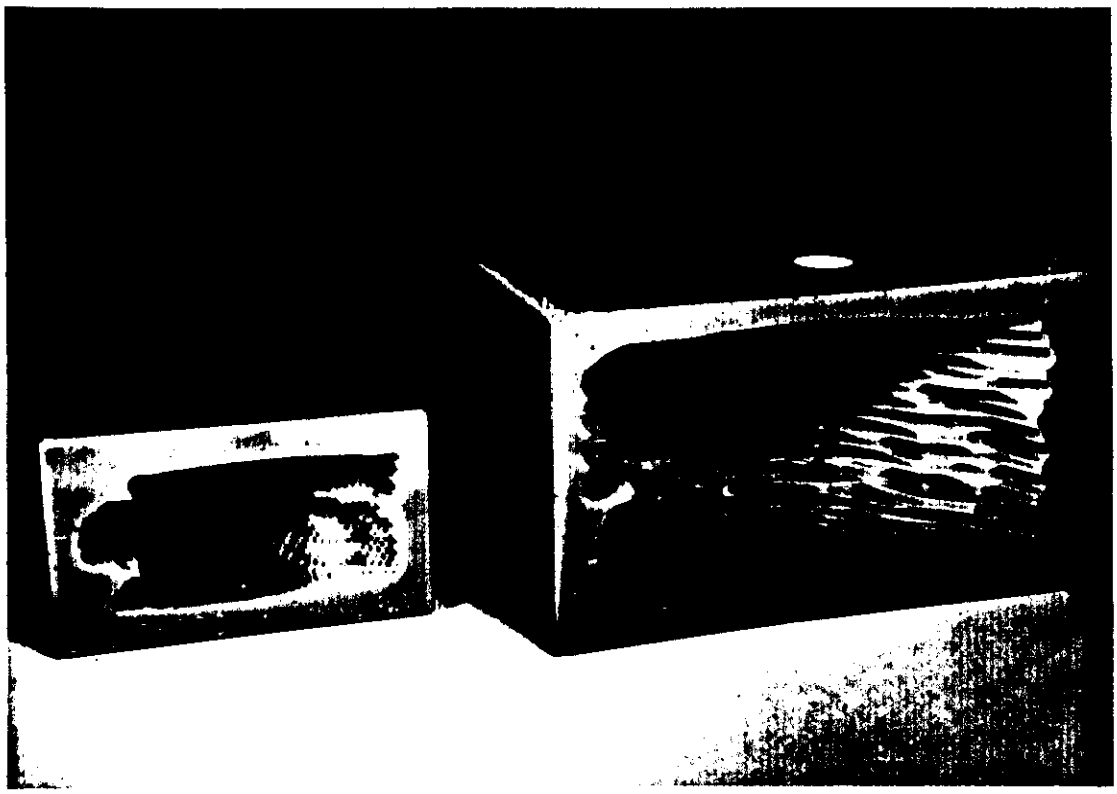

Figure 5: Examples of wax compensators used for charged-particle radiotherapy at LBL. The smaller compensator on the left side of the figure was designed for the treatment of a tumor situated at the skull base and thus exhibits more structure than the compensator on the right, which was designed to treat a region of the body where there are fewer heterogeneities.

Range Modulation

Although one of the first clinical applications of proton beams was to treat small pituitary lesions (35), the Bragg peak itself is rarely used clinically because its width is far smaller than that of an average-sized tumor. To treat large lesions, one must "modulate" the beam's range. This is most commonly done with a variable thickness absorber such as the propeller or bar-ridge filter shown in Figure 6. Charged-particle beams may also be modulated dynamically during the treatment (36).

Wilson was the first to propose the use of propellers (1, 37), and Koehler et al later described a working system (38). As the blades of the propeller rotate through the beam, the ranges of particles that penetrate different amounts of plastic are shortened correspondingly. The resulting beam is the superposition of Bragg peaks with different ranges, as illustrated in Figure 7. Propellers are usually made of relatively low-Z materials such as Lucite, to minimize multiple scattering. By choosing the angular width of each blade appropriately, the spread-out Bragg peak can be made uniform to within 2%. Propellers have been used as range-modulating devices at the Harvard Cyclotron Laboratory (HCL) (38, 39), the Loma Linda University Medical Center (LLUMC) (40), and at LBL (41-43).

Ridge filters such as the one shown in Figure 6b are made of heavy metals (e.g. brass) and consist of a series of closely spaced wedges. These devices are used primarily for heavy-charged particles (e.g. neon ions). High-Z materials are preferred for heavy-ion beam modulators because fragmentation of the incoming particle is less likely in high-Z than in low-Z materials. For the brass ridge filters, the mixing of particles with different ranges is accomplished through multiple scattering.

Whichever technique is used to modulate a charged-particle beam, the dose D at some depth x as a result of superimposing Bragg peaks is given by $D(x) = \sum w_i B_i(x)$, where $B_i(x)$ represents the depth-dose distribution for a Bragg curve with range equal to R_i, and x is the depth in water. Given the individual Bragg curves, an iterative procedure, such as the one described by Koehler et al (38) is most commonly used to solve for the beam weights, $\{w_i\}$. These weights are then used to specify the widths of the propeller blades or the ridge shape.

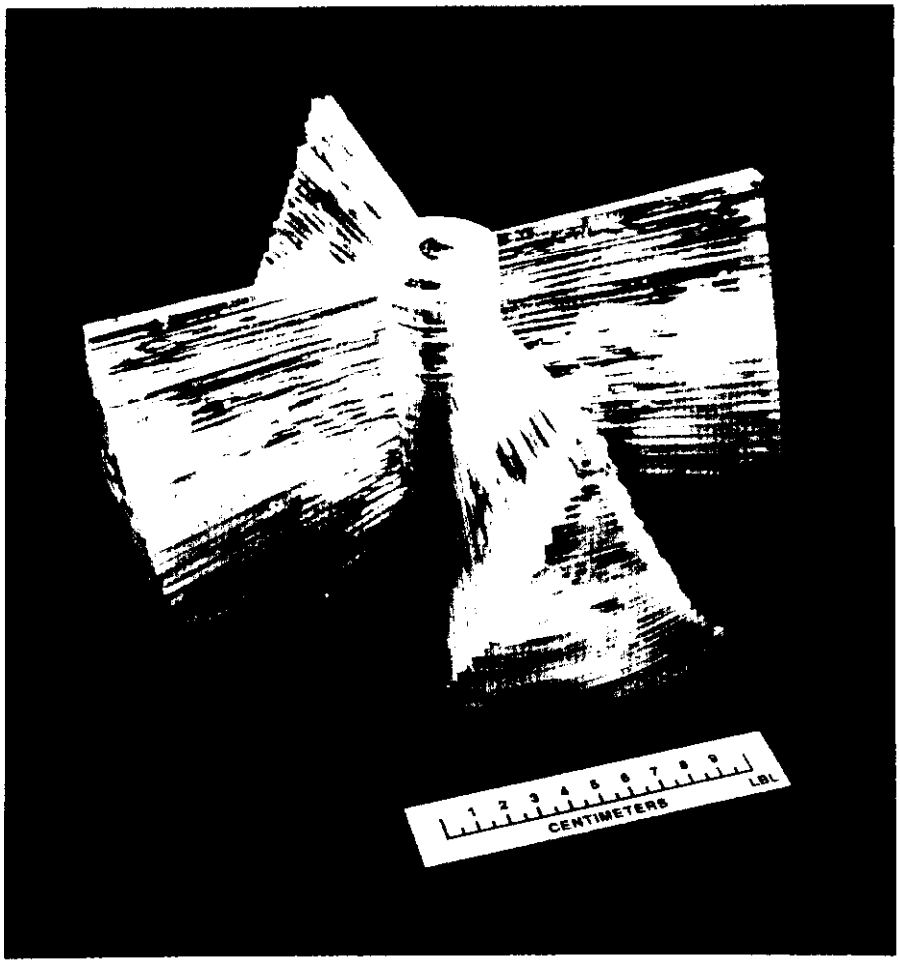

Figure 6a A Lucite propeller used for helium-ion treatments at LBL. This propeller was designed to create a 14-cm spread-out Bragg peak.

Dose Calculations

To calculate the dose at any point in the patient, one must first determine the water-equivalent distance to the point in question from CT data. The appropriate dose is then extracted from a lookup table compiled from measurements made in a water-equivalent phantom. These calculations are one-dimensional in that they neglect multiple Coulomb-scattering effects in complex heterogeneous regions, but they suffice in many clinical applications. One way to describe adequately the effects of multiple-Coulomb scattering is to model the beam in terms of differential pencil-beam contributions (7). Using this technique, the dose at a given point as a result of primary and scattered particles is determined by superimposing the contributions from pencil beams summed over the entire beam area. The differential pencil-beam dose distribution, $F(r,x)$, is defined as the dose deposited by an infinitely narrow beam in a homogeneous water phantom in an annular ring between depths x and $x + dx$ and radii r and $r + dr$. $F(r,x)$ may be determined by a combination of measurements and Monte Carlo calculations. The dose, D, at any point, P, in a *heterogeneous* geometry is:

$$D_P = D_0 \int_0^{r_{max}} r dr \int_0^{2\pi} \frac{F(r,x)}{2\pi r} \Phi(r,\theta) d\theta \ , \qquad (3)$$

where D_0 is the prescribed or maximum dose, $\Phi(r,\theta)$ is the beam intensity distribution, x is interpreted as the water-equivalent pathlength to each point (r,θ), and r_{max} is the maximum distance over which scattered particles contribute to the dose. The distance, r, and angle, θ, are measured about point P.

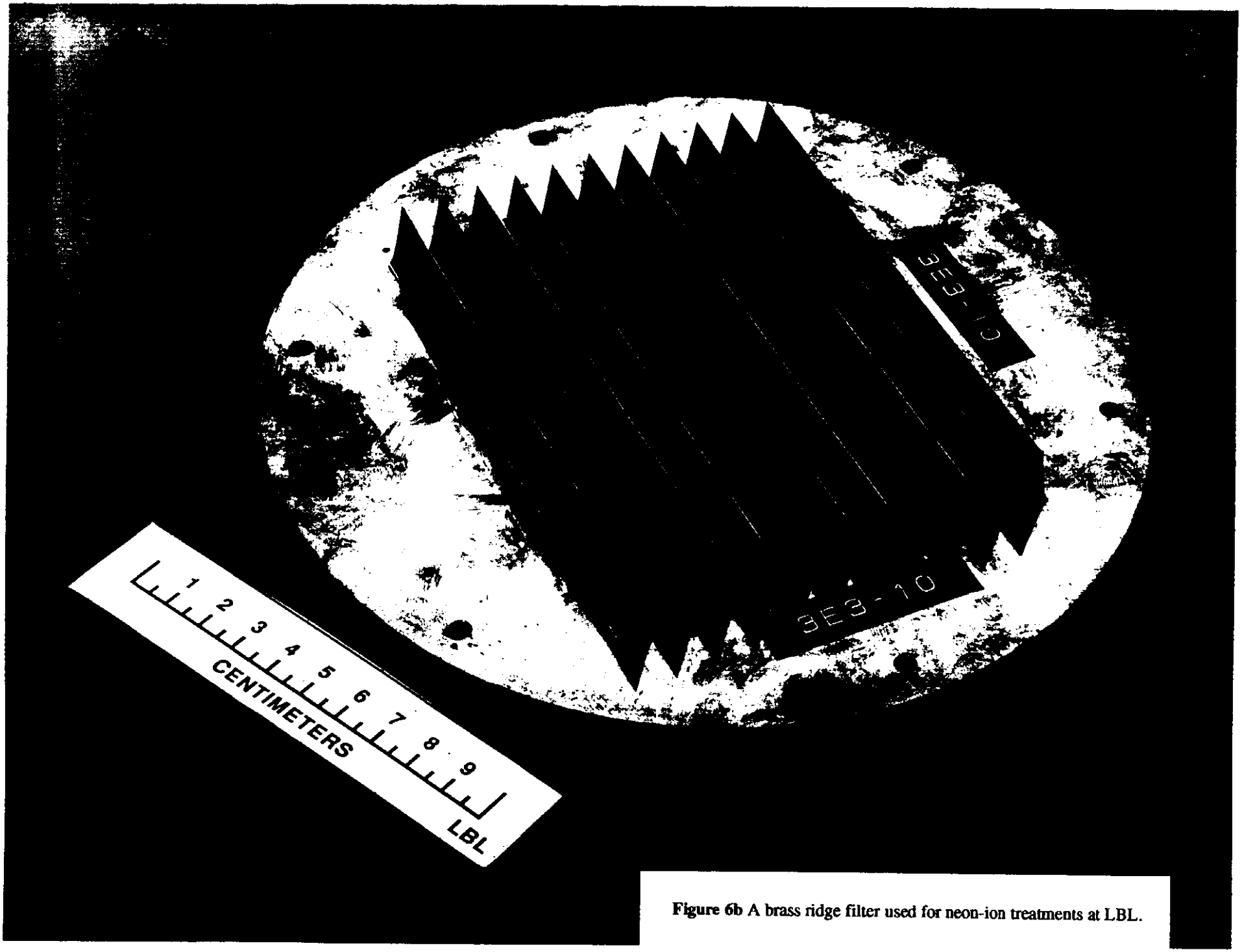

Figure 6b A brass ridge filter used for neon-ion treatments at LBL.

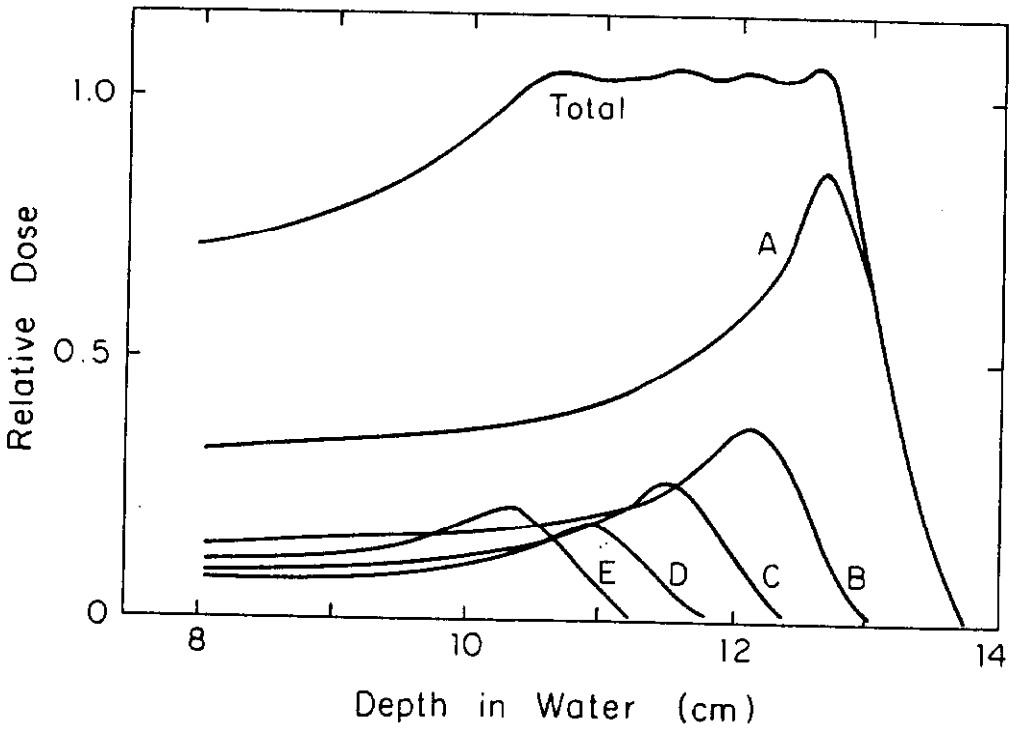

Figure 7: A schematic diagram illustrating how Bragg peaks with different ranges are superimposed to achieve a spread-out or modulated Bragg curve. Note that the most penetrating beam is given the largest weight. Redrawn from reference 39.

Treatment Planning for Charged-Particle Therapy

The first step in the treatment planning process for charged-particle radiotherapy is to obtain a CT scan of the patient immobilized in the treatment position. Because the alignment of the compensator with respect to the patient is crucial, rigid patient immobilization is required, and each patient must be fitted with a customized immobilizing device. For head and neck cases, this device usually consists of a mask made of thermoplastic material that is fabricated individually for each patient (Figure 8). Using computer graphics techniques, the physician outlines the tumor volume as well as critical structure volumes on all relevant CT slices (Figure 9). Magnetic Resonance imaging (MRI) is also frequently used to identify the tumor volume, and image-correlation techniques (44 - 48) are employed to transform volumes of interest from the MRI to the CT image. Collimators for each beam direction used in the treatment are then designed by projecting the tumor volume and critical structure volumes in the "beam's eye view" (49). This concept is illustrated in Figure 10 in which the tumor volume has been projected on a digitally reconstructed radiograph in the coronal (i.e. frontal) plane. (A digitally reconstructed radiograph is obtained by integrating the CT data along rays directed from a specified source point to the observer. The result is a planar projection of the CT data that resembles a planar radiographic image.) The inner outline on Figure 10 is the projected tumor volume determined from the outlines drawn by the physician on the axial CT slices. The outer outline represents the beam collimator and is obtained by adding an appropriate margin around the projected tumor volume to account for the beam penumbra as well as the possibility of patient motion during treatment. Once a set of suitable beam orientations is chosen and collimators and compensators are designed for each of these beam directions, the total dose distribution is calculated in the patient.

Figure 11 shows an example of such a distribution displayed on an axial CT slice. In this example, although three of the five beam directions used in this treatment are aimed at the brain stem, the dose at the center of the brain stem is only 10 - 30% of the maximum tumor dose. Another example of how protons or helium ions can be used to treat tumors situated near critical normal structures is shown in Figure 12. In this case, the tumor surrounds the spinal cord. To treat the tumor with a therapeutic dose while limiting the spinal cord dose to a tolerable level, the anterior part of the tumor is treated with beams directed toward the patient's left and right, whereas the posterior portion of the tumor is treated with a beam directed posteriorly and compensated so that the beam stops before reaching the spinal cord. In this case, the spinal cord dose was limited to 10% of the prescribed tumor dose. Castro et at described this divided-target technique and its results for 47 patients (50).

Figure 8: A patient is fitted with customized immobilization prior to treatment. In this case, the patient is immobilized with both a body cast and a head mask.

Figure 9: To design an optimal treatment plan with compensated beams, the physician must first outline the target volume and critical structures on all relevant slices of an axial CT scan.

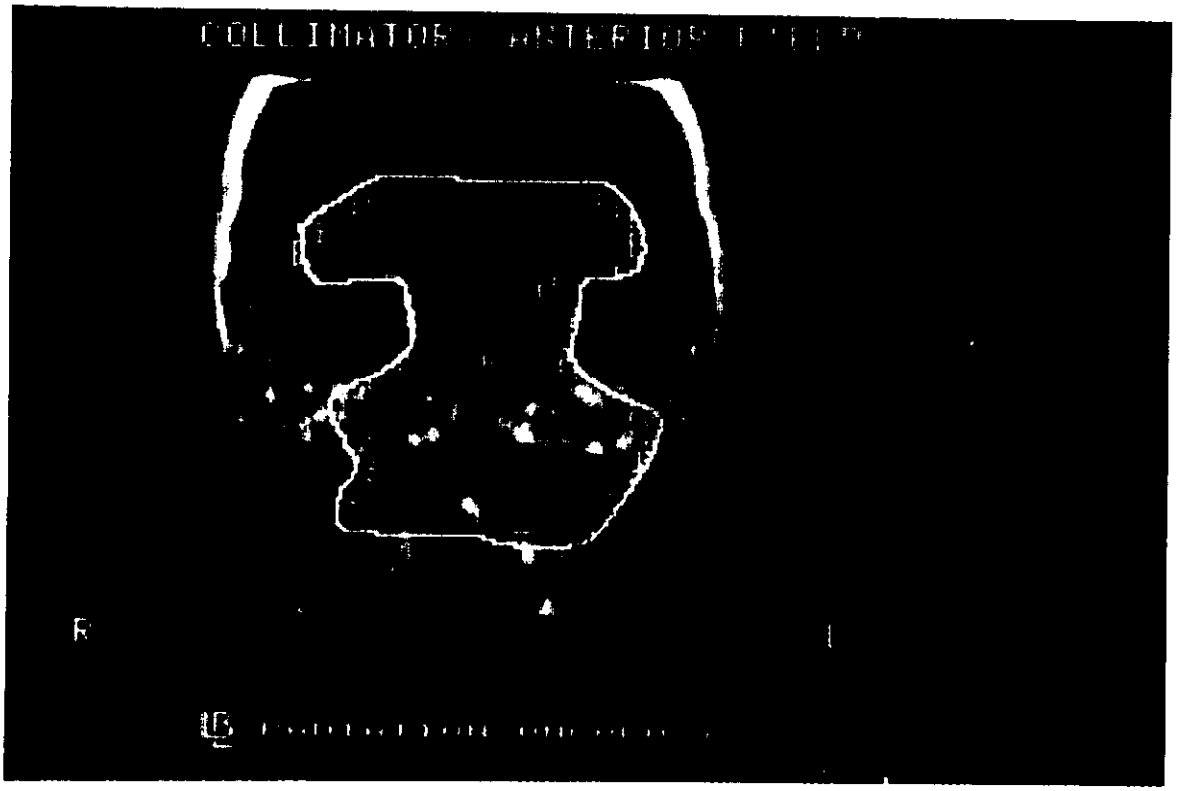

Figure 10: Collimators are designed for each beam direction used in the treatment by projecting the contours drawn by the physician in the plane orthogonal to the beam direction. In this case, the projected contours are superimposed on a coronal digitally reconstructed radiograph in order to design a collimator for a beam directed towards the patient's face. Note that the collimator is shaped to avoid irradiating the patient's eyes to the greatest extent possible.

Tailoring the dose distribution to the target volume using several beam directions with beam's eye-view collimators, for example, is called *conformal radiotherapy.* Many of the techniques and ideas developed specifically for and essential to charged-particle radiotherapy are now also being used to implement conformal photon radiotherapy. These include the use of CT and MRI data to delineate target and critical structure volumes, the beam's eye-view representation of these structures, and a detailed three-dimensional description of the dose distribution.

Clinical Results with Protons and Helium Ions

Since Wilson first proposed using charged particles therapeutically, more than 12,000 patients have been treated worldwide (51). Clinical results for the treatment sites studied to date are summarized below.

SKULL-BASE TUMORS: For skull-base tumors such as chordoma, chondrosarcoma, meningioma, craniopharyngioma, and pituitary adenoma, the ability to deliver an adequate dose using standard photon radiotherapy techniques is often limited by the proximity of these tumors to critical structures such as the brain stem, temporal lobes, optic chiasm, and optic nerves (52). New conformal photon therapy techniques that rely on modulating the beam intensity dynamically may eventually be useful in treating these tumors. However, these techniques have not been fully tested clinically. With standard photon therapy, one generally can deliver only about 50 Gy to such tumors, whereas with helium ions or protons, doses as high as 70 Gye are routinely used. (The term Gye stands for Gray-equivalent or effective dose, which is obtained by multiplying the physical dose delivered by the RBE for the particle in question.) Using conventional radiotherapy, the 3-year local-control rate for chordoma and chondrosarcoma is roughly 40%, while for proton therapy, the 5-year actuarial local-control rate for these tumors is 82% (53). The reported overall 5-year actuarial local-control rate for helium-ion irradiation of chordoma is 63%, while for chondrosarcoma it is 85% (54, 55).

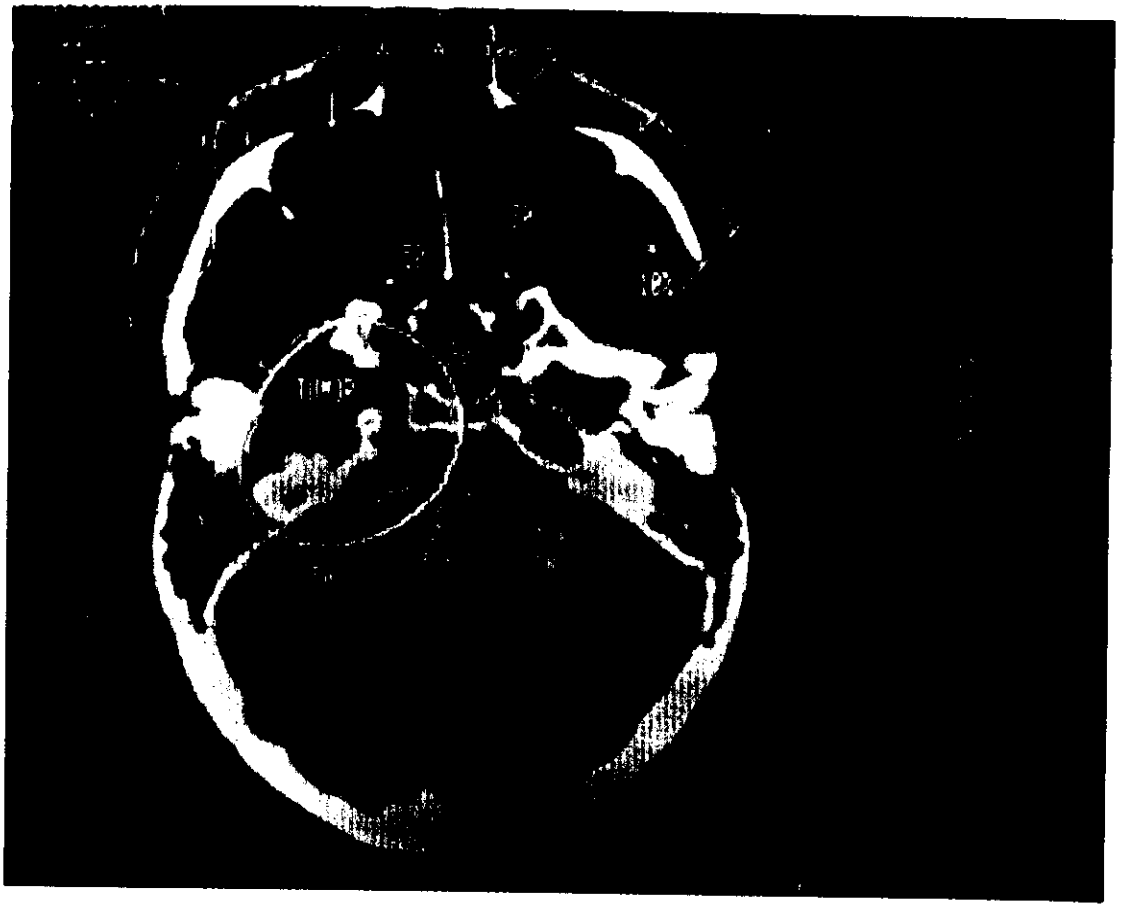

Figure 11: Example of a treatment plan for a clival chordoma, a rare congenital tumor located at the skull base. The heavy outline represents the tumor volume, whereas the lighter lines are the isodose contours. The isodose contours represent percent of the maximum dose. Five beam directions, indicated by arrows, were used in this plan to avoid delivering excessive doses to the brain stem (dotted line).

UVEAL MELANOMA: Protons and helium ions have been used to treat uveal melanoma, a tumor made of melanin-pigmented cells occurring in the vascular middle coat of the eye, comprising the iris, ciliary body, and choroid. Depending on the exact location of the tumor, this approach can avoid irradiating critical structures in the eye such as the optic disc, macula, and lens, as illustrated schematically in Figure 13. The goal of these treatments is to destroy the reproductive capacity of the tumor while preserving whatever vision the patient may have in the affected eye. The conventional treatment for these tumors is enucleation (i.e. removal) of the affected eye.

Currently, the only other form of radiation therapy for uveal melanoma to which particle therapy can be compared is irradiation with radioactive plaques (56). A radioactive plaque is made by gluing radioactive seeds (e.g. I-125) to a gold backing. The seeds and the backing are then affixed to a plastic disk similar in shape to a contact lens, which is fabricated individually for each patient to fit his or her eye. The entire assembly is then sutured to the patient's eye over the tumor and remains in place until the desired dose is delivered. The rate of local failure (i.e. continued tumor growth) observed with charged particles appears to be less than that reported for radioactive plaques (57). Various groups using different forms of radioactive plaques report local failures leading to enucleation in 10% - 40% of the patients treated (58 - 63). In contrast, both the groups at the Massachusetts General Hospital (MGH) in Boston (64) and at LBL (65, 66) report 5-year actuarial local-control rates of at least 97%. However, a small number of patients (< 2% in the LBL series) required enucleations due to continued tumor growth or regrowth. Approximately 10% of the patients in both the MGH and LBL series underwent enucleations because of radiation-induced complications such as neovascular glaucoma. The 5-year actuarial eye-retention rate reported by Linstadt et al (65) for helium-ion irradiation at LBL was 83%, whereas Munzenrider et al (67) and Egan et al (68) reported a 5-year actuarial eye-retention rate of 89% for proton therapy at MGH.

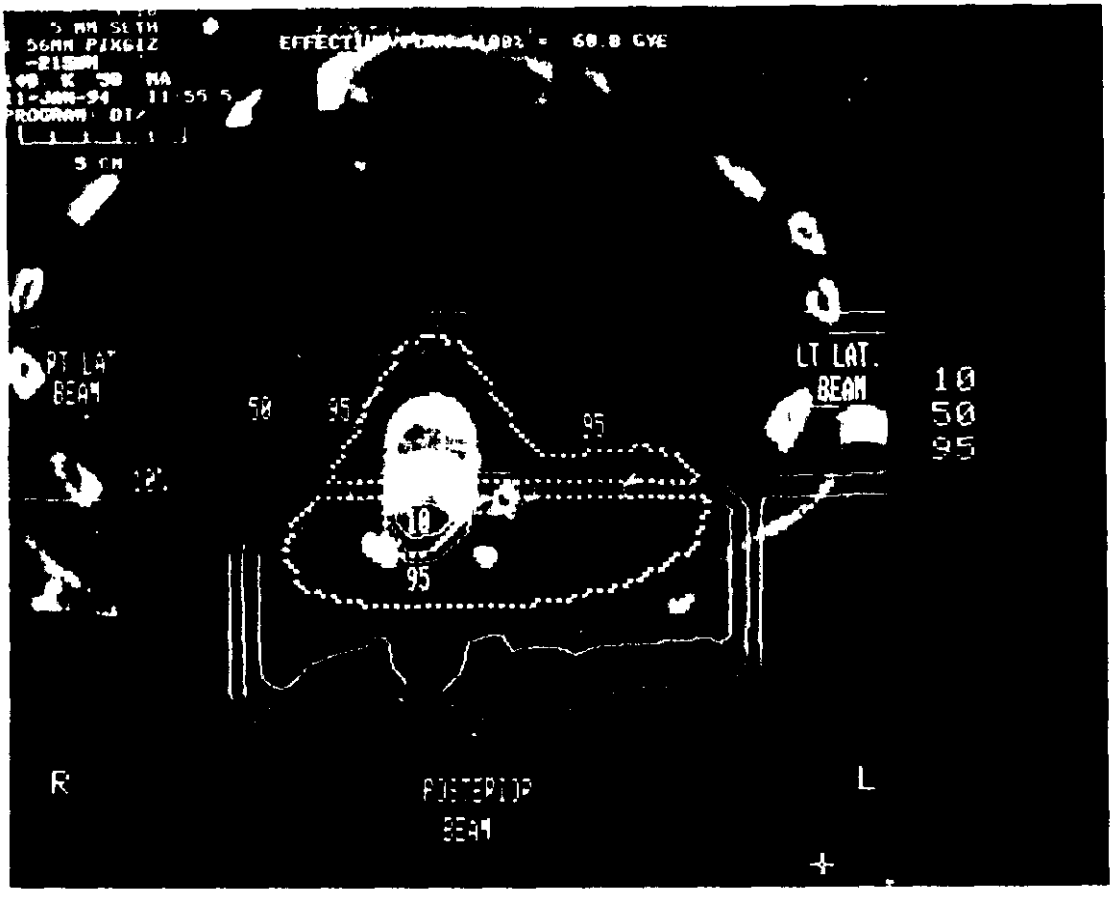

Figure 12: Example of a divided target treatment plan. The target is divided into anterior and posterior sections. The anterior portion is treated with opposed lateral beams, whereas the posterior portion of the target is treated with a posterior beam designed to stop just before reaching the spinal cord. The isodose contours represent percent of maximum dose.

ARTERIOVENOUS MALFORMATIONS (AVMS): An arteriovenous malformation is a set of tangled and malformed blood vessels in the brain that is at risk for hemorrhage. AVMs may be surgically removed, embolized, or treated with radiation using conformal techniques. At the HCL, Kjellberg has treated more than 1300 AVM patients (69 - 75) and reports that 91% of 896 AVM patients treated with protons showed the same or improved neurologic status following treatment. The 24-year actuarial survival rate for this group of patients was 98% for those with AVMs greater than 3 cm in diameter and 93% for all patients. For an untreated control group, the 24-year actuarial survival rate was 77% (76).

More than 400 patients with surgically inaccessible AVMs were treated with helium ions at LBL between 1980 and 1990 (69). The complete angiographic obliteration rate (i.e. the disappearance of the AVM upon angiographic examination) 3 years posttreatment for this group of patients was 90% - 95% for those with AVM volumes < 14 cm^3, and 60% - 70% for those with volumes > 14 cm^3. The overall obliteration rate for all volumes (as large as 70 cm^3) was 80% - 85%. At the Burdenko Neurosurgical Institute for Theoretical and Experimental Physics (BNI-ITEP) in Moscow, Minakova and colleagues have treated 66 AVM patients with protons between 1983 and 1990 (77 - 79). Of these patients, 28 had follow-up angiographic studies, which revealed a complete or partial obliteration rate of 71%.

AVMs are also treated effectively with specialized conformal techniques using photons, i.e. gamma-knife or linac radiosurgery. It is beyond the scope of the review to describe these techniques in detail, and we refer the interested reader to reference 80 for more information. In general, the dose distributions for small lesions are essentially equivalent for the photon and charged-particle techniques, whereas for large irregularly shaped lesions, one can obtain superior dose distributions using particles. However, clinical results for all of these techniques are comparable.

TREATMENT SITES WITHIN THE THORAX, ABDOMEN, AND PELVIS: Limited clinical studies have been performed with protons and helium ions for sites outside of the head and neck region. Early trials of helium-ion radiotherapy for locally advanced esophageal, pancreatic, and biliary tract carcinoma were conducted at LBL (81, 82). More recently, Tsujii et al at the Proton Medical Research Center at the University of Tsukuba in Japan have reported preliminary results for proton radiotherapy for 147 patients (83). Most of the patients in this study received large total doses (> 70 Gy). Indications of improved local-control and survival rates were found for lung, esophageal, liver, uterine cervix, and prostate cancers. Some of these results, in particular those for esophageal carcinoma, contradict earlier findings reported by Castro et al (82) who observed no improvement in local-control rates over conventional photon therapy. These differences have been attributed to the higher total doses used by the Japanese group (70 - 87 Gye vs to 62 - 70 Gye in the study by Castro et al) and to improved techniques for identifying the tumor volume.

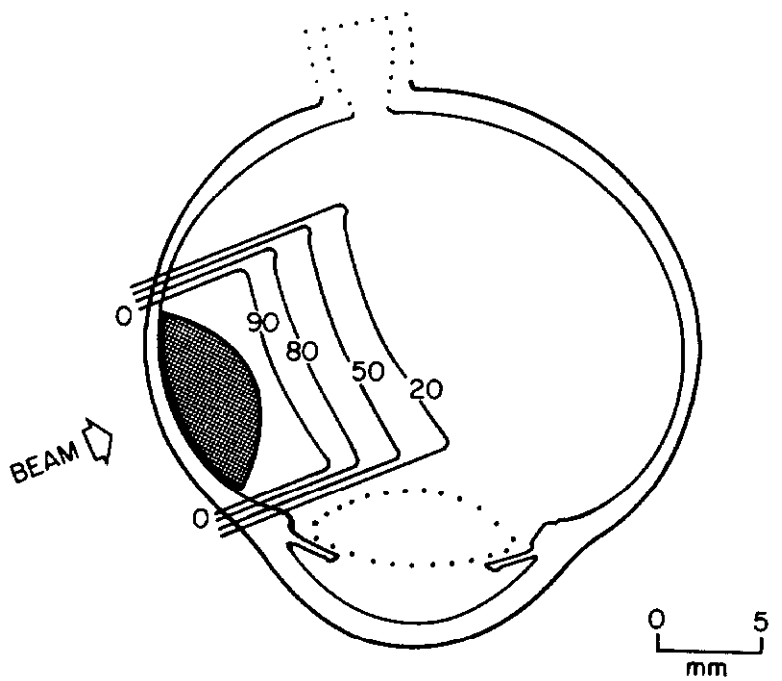

Figure 13: A schematic illustration of how protons or helium ions are used to treat ocular melanoma. The goal of the treatment is to select a beam direction (or equivalently, a direction in which the patient gazes) so that the tumor is treated adequately and critical structures of the eye such as the lens, fovea, and optic nerve receive only minimal dose.

Treatment Centers and Accelerators for Proton and Helium-Ion Radiotherapy

Proton energies required for treating patients range from 70 - 250 MeV. Until the commissioning of the proton synchrotron at LLUMC in 1990, such energies were available only at accelerators built for basic physics research. Chu et al prepared a summary of radiotherapy centers that have been treating patients throughout the world (36). Table 1 lists these centers as well as the type of accelerator used and the maximum available energy. Patient totals in the table are from Fukumoto (S. Fukumoto, private communication). Accelerators with energies of 60-90 MeV are limited to treating tumors such as ocular melanoma, whereas those with higher energies can be used to treat deeper tumors.
In addition to the those listed in Table 1, several institutions are planning either a dedicated medical proton machine or a modification of an existing accelerator to accommodate medical applications. MGH is currently planning a dedicated hospital-based proton treatment center (84). The Indiana University Cyclotron Facility (IUCF) has developed a 200-MeV proton beam for clinical applications (85). Elsewhere around the world, the Paul Scherrer Institute (PSI) in Villigen, Switzerland, which formerly treated only ocular melanoma, is extending its program to include the treatment of deep-seated tumors (86), and the National Accelerator Centre in Faure, South Africa has developed a clinical proton beam line in addition to its neutron beam line (87). In Japan, a dedicated medical synchrotron has been designed at Tsukuba (88,

Table 1: Proton and Helium ion treatment centers. An asterisk indicates that the group used helium ions instead of protons.

Group	Location	Accelerator Type	Beam Energy (MeV/amu)	Dates	Patient Total (Date)
LBL (184")	Berkeley, CA	Synchrocyclotron	340	1954-1957	30
LBL* (184")	Berkeley, CA	Synchrocyclotron	230	1957-1987	3035
LBL* (Bevalac)	Berkeley, CA	Synchrotron	215	1988-1992	210
HCL, MGH	Cambridge, MA	Synchrocyclotron	160	1961-	5876 (7/93)
GWI	Uppsala, Sweden	Synchrocyclotron	185	1957-1976	73
TSL	Sweden	Cyclotron	200	1991	–
ITEP	Moscow, Russia	Synchrotron	70-200	1969-	2550 (5/92)
JINR	Dubna, Russia	Cyclotron	680	1964-1974	84
LINP	St. Petersburg, Russia	Synchrocyclotron	1000	1975-	719 (6/91)
NIRS	Chiba, Japan	Cyclotron	70	1979	86 (6/93)
PARMS	Tsukuba, Japan	Synchrocyclotron	250	1982	353 (7/93)
PSI	Villigen, Switzerland	Cyclotron	72	1984-	1363 (5/93)
MRCC, CH	Merseyside, England	Cyclotron	62.5	1989-	369 (5/93)
LLUMC	Loma Linda, CA	Synchrotron	250	1990-	535 (4/93)
CAL	Nice, France	Cyclotron	63	1991-	216 (4/93)
CPO	Orsay, France	Cyclotron	200	1991-	235 (4/93)
UL	Louvain-la-Neuve, Belgium	Cyclotron	90	1991-	14 (6/92)

The names are coded as follows: Lawrence Berkeley Laboratory (LBL), Gustaf Werner Institute (GWI), Harvard Cyclotron Laboratory (HCL), Massachusetts General Hospital (MGH), Theodore Svedbrerf Laboratory (TSL), Institute of Theoretical and Experimental Physics (ITEP), Joint Institute of Nuclear Research (JINR), Leningrad Institute for Nuclear Physics (LINP), National Institute of Radiological Sciences (NIRS), Particle Radiation Medical Science Center (PARMS), Paul Scherrer Institute (PSI), Medical Research Council Cyclotron Unit (MRCC), Clatterbridge Hospital (CH), Loma Linda University Medical Center (LLUMC), Centre Antoine-Lacassagne (CAL), Centre de Protontherapie d'Orsay (CPO), University of Louvain (UL).

89), and a 250-MeV AVF separated-sector cyclotron in Osaka University will be used partially for medical sciences applications (90). Additionally, the Institute of Theoretical and Experimental Physics (ITEP) in Moscow, Russia, is planning a dedicated proton synchrotron (91, 92), and the COSY/Jülich program of the German Forschungszentrum (KFA) is building a new 20-1000 MeV synchrotron, for which medical applications are planned (93). The Laboratori Nazionali di Legnaro (LNL) in Padova, Italy plans to develop a proton beam with energies between 20 and 1000 MeV which will have some medical applications (94), and the Tri-University Meson Facility (TRIUMF) in Vancouver, Canada plans to use protons with energies between 72 and 500 MeV for patient treatments (95). Finally, under the auspices of the Fondazione per Adroterapia Oncologica (TERA), the Italian government is planning a center for dedicated proton therapy in Novara, Italy (96).

Much work has been done to optimize accelerators for hospital-based treatments. Because the energy of a cyclotron is not easily varied, beam absorbers (e.g. water or polystyrene) are used to adjust the beam range. This inefficient use of the beam can be avoided by using a proton synchrotron to extract beam directly at the appropriate energies. If an H^- synchrotron is used, one can accelerate helium and heavy ions for therapy with the same accelerator (97). Finally, a proposal has been put forth to use commercially available S-band radiofrequency power systems and accelerating cavities to build a proton linac for proton radiotherapy (98). Ref. 99 contains an excellent discussion of accelerators for proton therapy as well as many other biomedical applications.

Proton Radiotherapy versus Conformal Photon Techniques

Clinicians must assess the improved dose-localizing ability of protons in light of the costs of building and maintaining a medically dedicated proton treatment center. New conformal radiation-therapy techniques for photons have emerged that make it possible to obtain photon isodose distributions which are competitive with proton treatment plans. The costs of implementing proton and conformal photon radiotherapy programs are most often compared in terms of the costs of the accelerators and associated hardware alone, which leads to the conclusion that the cost of proton therapy exceeds that of conformal photon therapy by approximately a factor of 10. However, one proton synchrotron can be used to supply beam to at least four treatment rooms. (The Loma Linda synchrotron services four treatment rooms and one room devoted to biological studies.) Moreover, the lifetime of a proton synchrotron has been estimated to be 25 - 35 years, while the lifetime for an electron linac is typically 10 - 12 years. Assuming that the number of patients treated per day per treatment room is approximately the same for conformal photon and proton techniques, these two properties of synchrotrons imply that, over the accelerator lifetime, between 8 and 14 times more patients can be treated with a proton synchrotron than with an electron linac configured for conformal photon therapy. This increased capacity compensates for the estimated factor of 10 difference in cost between the two types of machines.

HIGH-LET CHARGED PARTICLES

Accelerated heavy ions provide both the physical advantages of Bragg-peak radiotherapy as well as the radiobiological advantages of high-LET particles. Figure 14 shows an unmodulated Bragg curve for a 585-MeV neon beam. Although the width of the peak is narrower, the shape of the curve resembles a proton or helium beam. One important difference between the depth-dose distributions for heavy- and light-ion beams is that, for the heavy-ion beams, significant dose is deposited beyond the Bragg peak by particles produced in nuclear interactions between the incoming heavy ions and the atomic nuclei. For a neon beam, this tail dose is ~20% of the peak dose for a spread-out Bragg curve, and must be carefully considered when planning heavy-ion treatments.

The possibility of using neon, carbon, and silicon ions was investigated from 1977 until 1992 at LBL. Radiobiological studies indicated that the ratio of the effective dose in the peak to the effective dose in the entrance or plateau region was higher for carbon than for neon. This finding suggests that carbon ions are optimal because they deliver lower doses to normal tissues upstream from the tumor. Conversely, the OER was shown to be lower for neon and silicon ions than for carbon ions, which implies that, at least theoretically, ions with higher atomic numbers should be more effective therapeutically because most tumors are hypoxic. For this reason, neon ions with energies between 450 and 670 MeV per nucleon were selected for the heavy-charged particle radiotherapy research trials at LBL.

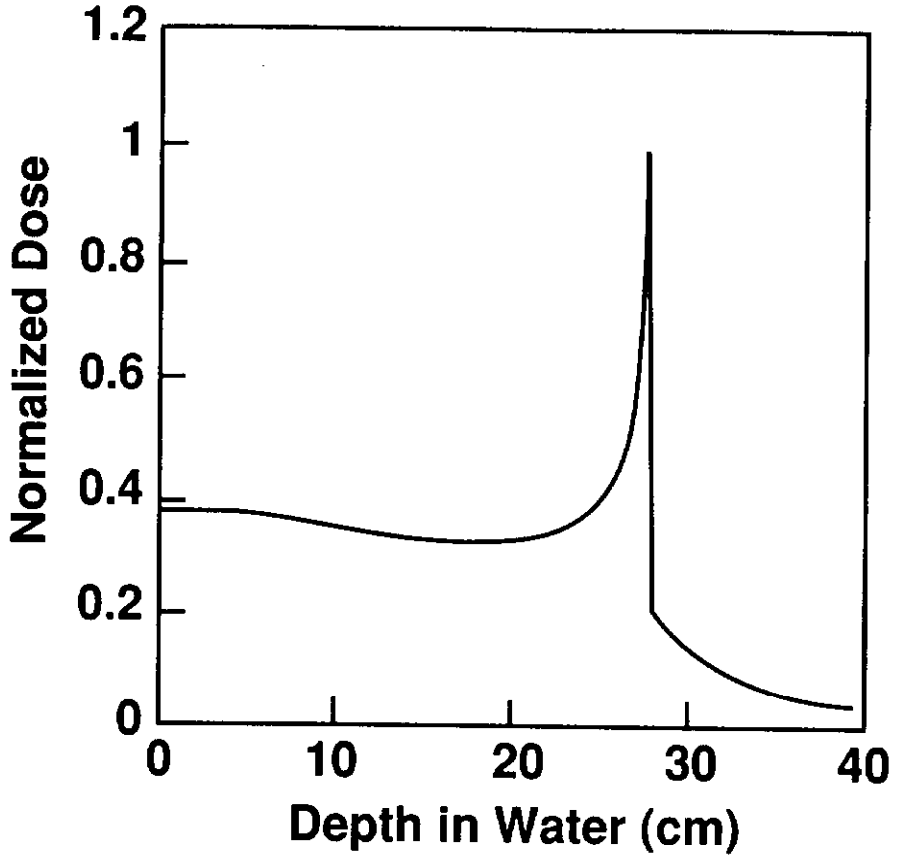

Figure 14: An example of a depth-dose curve for an unmodulated neon beam (585 MeV/amu) produced by the Bevatron at LBL.

Treatment Planning for High-LET Charged Particles

Treatment planning for heavy-ion radiotherapy is nearly identical to that for low-LET charged particles. The main difference is that the RBE for high-LET charged particles changes significantly as a function of beam penetration. The RBE is highest at the distal end of the spread-out Bragg peak, where the LET is the largest. To deliver a uniform effective dose to the tumor volume with heavy-ion beams, one must compensate for the variation in RBE across the spread-out Bragg peak by designing modulated beams such that the biological effect, as predicted by the linear-quadratic cell-survival model (100 - 103), is constant across the spread-out Bragg peak (41, 42). Figure 15 shows an example of a modulated neon beam designed to satisfy this criterion. The physical dose is lowest in the most distal portion of the spread-out Bragg peak where the RBE is the highest. However, the effective dose is constant across the spread-out Bragg peak.

Clinical Results using Neon-Ion Beams

Table 2 lists tumor sites for which neon-ion irradiation shows promise. This table compares local-control or survival rates achieved with neon ions to those reported for conventional photon radiotherapy. The number of patients treated in the neon trials is given in parentheses. These data were taken primarily from a paper by Linstadt et al that summarizes the results of clinical trials for neon-ion radiotherapy at LBL undertaken between 1979 and 1988 (104). They report results for 239 patients with various tumor histologies. By 1992, just before the Bevatron (LBL's heavy ion accelerator) closed, a total of 299 patients had received at least 10 Gy with neon ions as part of their treatment. Although only a small number of patients in each category were treated with neon ions, the improvement in local-control or survival rates was significant. These are the only clinical trials for heavy charged-particle radiotherapy that have been carried out to date.

Tumors that showed no improvement in local-control rates over conventional radiotherapy in the LBL series include malignant glioma, melanoma, advanced or recurrent head and neck squamous-cell carcinoma, non-small-cell lung cancer, and esophageal, gastric, and pancreatic malignancies. However, as Linstadt et al

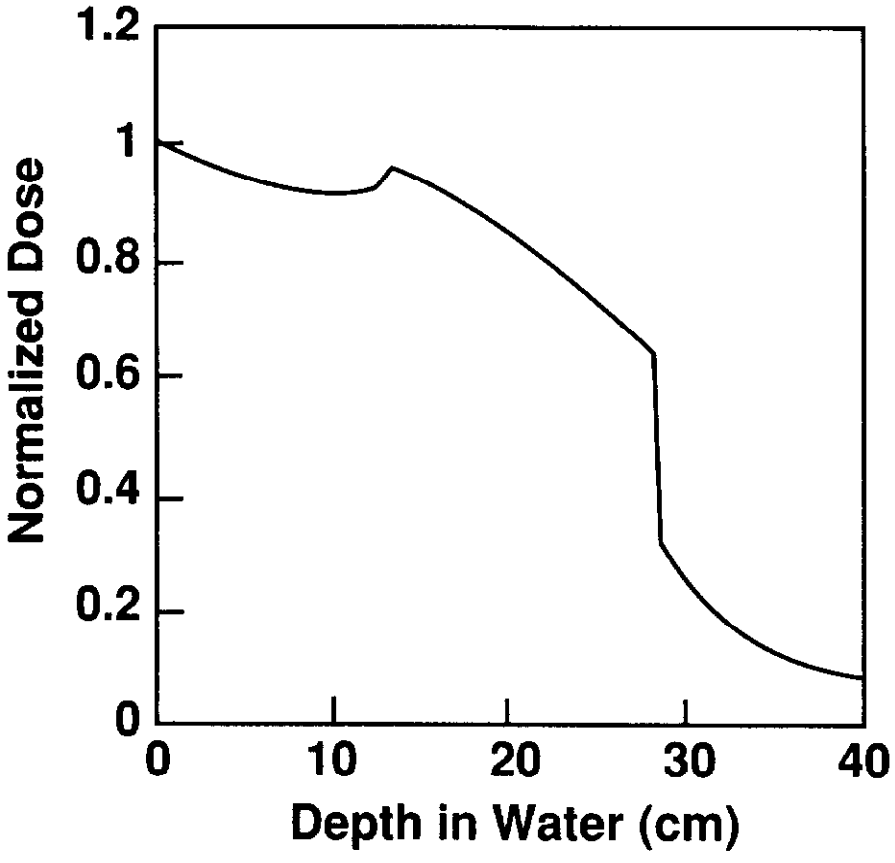

Figure 15: Example of a modulated neon beam. The width of the spread-out Bragg peak in this case is 15 cm. The dose is higher at the proximal part of the spread-out Bragg peak than it is at the distal end of the curve to compensate for the more severe radiobiological effects, which result from the higher LET, at the distal end of the curve.

pointed out, many of these patients were treated early in the clinical trial at a time when treatment techniques were still developing and optimal treatment doses were unknown. In addition, most of these patients had advanced disease for which no other form of curative therapy existed.

The results summarized in Table 2 are interesting in several respects. First, similar results have been reported for neutrons for many of these tumor types. In particular, locally advanced salivary gland tumors, soft-tissue sarcoma, and bone sarcoma all respond favorably to neutrons (104 and references therein), which suggests that the high-LET character of the heavy-ion beam and not its dose-localizing ability is the determining factor for these sites. Second, many of these tumors, e.g. biliary tract carcinoma tend to proliferate slowly. Laramore et al (26) and Batterman et al (105, 106) reported experimental evidence that slowly growing tumors have higher RBE values for neutron irradiation relative to ^{60}Co than do more rapidly growing tumors. This improved response is attributed to the decreased variation in radiosensitivity throughout the cell cycle phases for high-LET particles. Finally, Table 2 contains examples of rapidly growing tumors (e.g. osteogenic sarcoma) as well as slowly proliferating malignancies. For these tumors it has been suggested that high-LET radiation is advantageous because rapidly proliferating tumors outgrow their blood supply and become hypoxic. High-LET particles may have an advantage under these circumstances because of their low OER. In view of these results, Linstadt et al (104) have suggested that predictive assays (i.e. in vitro tests using biopsy samples of the tumor) be performed for individual patients to determine the proliferation rate of their tumors so that those who stand to benefit the most from heavy-charged particle radiotherapy might be selected.

One should also consider the response of normal tissues to high-LET radiation. Just as high-LET radiation appears to be selectively damaging to slowly growing tumors, it also selectively injures slowly proliferating normal tissues, particularly those of the central-nervous system (CNS). For example, the neon RBE for brain tissue is believed to be between 4.0 and 4.5. The neon RBE for malignant glioma is

also in this range. When treating these tumors, one must take extreme care to avoid treating healthy brain tissue to doses in excess of ~10 Gy of neon (i.e. ~40 - 45 Gye).

The results of the neon-ion radiotherapy trials at LBL indicate that heavy-charged particles can be used to treat human malignancies safely and that they may be more effective than photons for the specific tumor sites listed above. However, several areas warrant further investigation, e.g. the optimal fractionation scheme for high-LET charged particles. For photons, it is advantageous to use fraction sizes of ~2 Gy per day. However, this strategy is probably not optimal for heavy ions. For high-LET particles, the RBE for small doses per fraction is greater than the RBE for larger fraction sizes because of the inability of cells to repair high-LET radiation damage. Thus, using a smaller dose per fraction does not help protect healthy normal tissues as is the case for photon therapy. In fact, evidence indicates that the effect of many small fractions of high-LET radiation is to injure normal tissues, particularly those of the CNS (12). By increasing the dose delivered per fraction with high-LET radiotherapy, the overall treatment time can be shortened to two or three weeks. This approach is advantageous because it minimizes the probability of tumor proliferation during the course of the treatment (12). Most of the clinical neon-ion trials at LBL used conventional fractionation schemes (i.e., 2 Gye per fraction or 0.7 - 0.8 Gy of neon). Only toward the end of these investigations were larger doses per fraction employed and, although too few patients were treated in this manner to draw any general conclusions, it was apparent that fraction sizes can be increased safely to about 2.0 Gy of neon (~5 Gye for photon irradiation) (JR Castro, personal communication).

Table 2: Tumor Sites that show promise for neon-ion radiotherapy. Results for conventional photon radiotherapy are also given. The bulk of these data are from Linstadt et al. (104). The number of patients treated in the neon trials is given in parentheses.

Disease	End Point	Neon Ions	Photons
Locally Advanced Prostate Cancer	5-yr local control	93% (23)[a]	50-60%
Inoperable and Recurrent Salivary Gland Carcinoma	5-yr local control	61% (18)	25 - 36%
Advanced Sarcoma of Soft Tissue	5-yr local control	56% (12)	30 - 50%
Sarcoma of Bone	5-yr local control	59% (19)	21 - 33%
Bilary Tract Carcinoma	5-yr local control	44% (8)	20%[b]
Macroscopic Paranasal Sinus Carcinoma	Long-term survival	69% (12)	32- 40%

[a] Castro, JR, private communication.

[b]This result is reported by Schoenthaler et al. (107) and describes the 2-yr actuarial local-control rate.

Treatment Centers and Accelerators for Heavy Ions

With the closing of the Bevatron at LBL in 1992, research with heavy ions was suspended. The Gesellschaft für Schwerionenforschung (GSI) in Darmstadt, Germany and the National Institute of Radiological Science (NIRS) in Chiba, Japan plan to treat patients with heavy ions in the near future. The German proposal uses a parasitic beam from the GSI synchrotron in collaboration with the University Clinic of Radiology in Heidelberg and the German Cancer Research Center (DKFZ). Treatment of patients is expected to begin in 1996 (108). In Japan, the Heavy Ion Medical Accelerator at Chiba (HIMAC) is a synchrotron dedicated to heavy-ion therapy (109). Patient treatments should start in 1994.

Some groups mentioned in the section on proton therapy plan to develop heavy-ion therapy after implementing proton therapy. These include the German COSY/Jülich project and the Italian TERA project. In Austria, plans are underway to implement heavy-ion and neutron-capture therapy (the AUSTRON project) (110).

NEGATIVE PION THERAPY

In addition to the Bragg peak, negative pions also exhibit a unique phenomenon called stars that makes them particularly attractive for treating radioresistant tumors. As a negative pion slows down near the end of its trajectory in tissue, it can be captured by one of the constituent atoms such as carbon, oxygen, or nitrogen, cascade down the atomic levels, and then be absorbed by the nucleus. The 140-MeV pion rest mass energy then appears as kinetic energy of the fragments produced when the nucleus disintegrates into a star of alpha particles, neutrons, and protons. The star phenomenon does not occur for positive or neutral pions, so only negative pions have been investigated for therapy. For the rest of this discussion the term pion refers only to negative pions.

Accelerators and Beam Delivery for Pions

Pions for therapy are produced by protons with energies > 400 MeV striking a beryllium or graphite target. Linacs, cyclotrons, and synchrotrons can be used to accelerate the protons. Negative pion beams are contaminated by electrons produced in the target and by muons resulting from negative pion decay. Beam lines that minimize contamination can be designed, but the unwanted particles cannot be removed completely, and their effects must always be considered.

Figure 16 shows the relative pion, electron, muon, and star contributions to the dose for a 190-MeV/c negative pion beam. In this figure, the energy deposition in the plateau between 0 and ~20 cm results from low-LET ionization losses, whereas the dose at the end of the pion range is due to relatively high-LET radiation from the stars. Thus, pion therapy has the advantage of low-LET dose to healthy tissue in the plateau region upstream from the tumor and high-LET dose at the end of the beam range in the tumor. Although stars provide a biological advantage, they seriously complicate pion dosimetry. In his excellent review of the early radiobiological work and dosimetry (111), Raju pointed out that the RBE changes with tumor volume, dose rate, and fractionation. This variation is attributed to the change in neutron production in different volumes. In addition, the electron and muon contamination change when modulators and boluses are used, which makes the development of a standard, easily applied dosimetry technique very difficult.

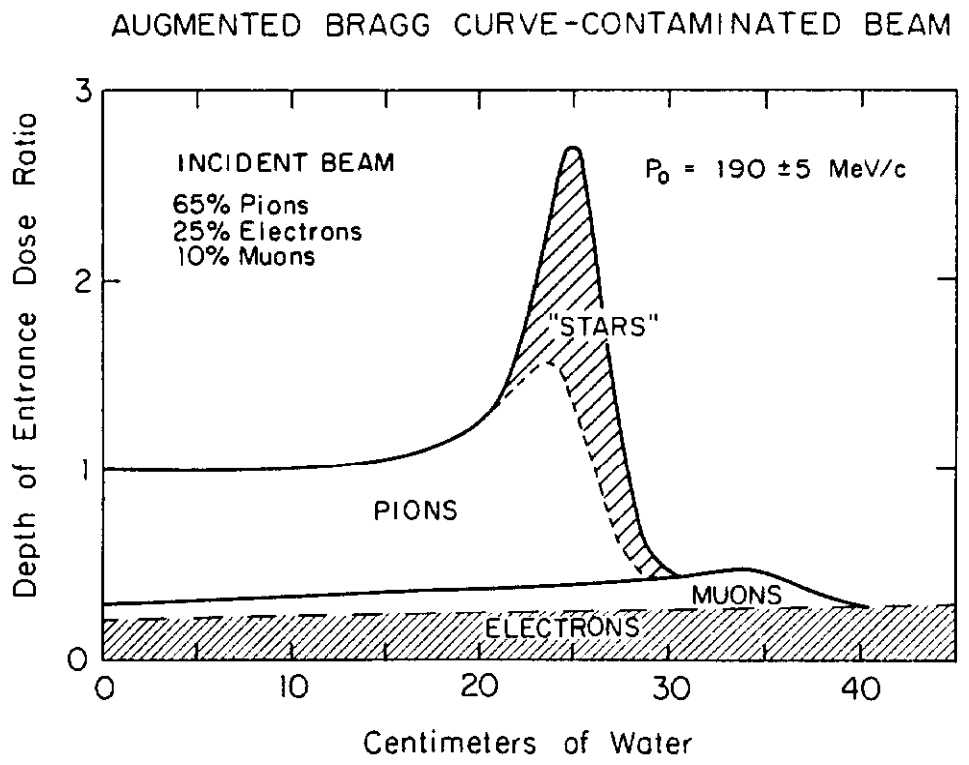

Figure 16: Depth-dose curve in water for a 190 MeV/c negative pion beam. Redrawn from reference 112.

A solution to the dosimetry problem was implemented at PSI in Villigen, Switzerland, where as many as 60 identical pion beams were arranged to stop on the axis of a cylindrical phantom, as shown in Figure 17. This resulted in a ~1-cm diameter spot whose radiobiological characteristics were well known. Patients were then treated by moving the tumor through the beam spot so that all parts of the tumor were irradiated by a beam with well-understood biological properties. The device used to administer dynamic pion therapy in this manner was called the PIOTRON (113). Its design, based on the Stanford Medical Pion Generator (114), minimizes the primary beam current requirements by providing a large solid-angle acceptance for pions from the production target. Thus, even though the work at Stanford never proceeded to clinical trials, it contributed significantly to the clinical trials at Villigen. Similarly, work done at Los Alamos to provide a high-intensity linac for hospital-based pion therapy (PIGMI) never reached the point of clinical trials, but developments on the radiofrequency quadrupole linac (RFQ) for that accelerator contributed to the development of the RFQ now used as an injector for the hospital-based proton synchrotron at LLUMC.

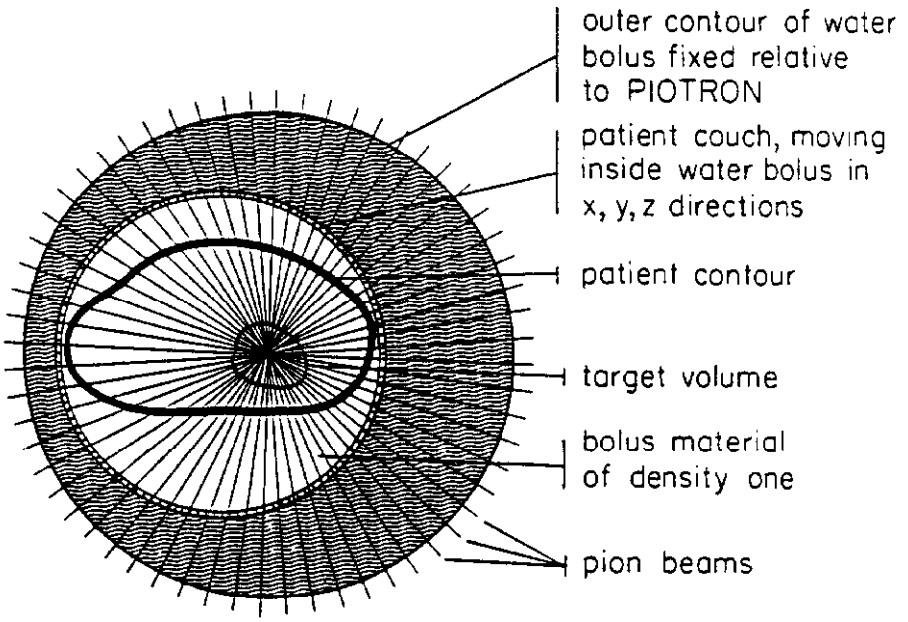

Figure 17: A schematic illustration of the dynamic therapy technique for negative pion therapy used at the PSI PIOTRON (Courtesy of H. Blattmann).

Clinical Trials for Pions

Clinical trials have been conducted at the Los Alamos Meson Physics Facility (LAMPF) in Los Alamos, New Mexico; PSI in Villigen, Switzerland; and TRIUMF in Vancouver, British Columbia. LAMPF treated 230 patients from 1974 to 1982 (51) and had used dynamic treatments for only a short time before funding was terminated. Just over 500 patients were treated at PSI between 1980 and 1993 with dynamic therapy to conform the dose distribution to the tumor volume (H Blattmann, personal communication). PSI has since stopped pion trials to concentrate on building a clinic to treat deep-seated tumors with protons. TRIUMF started treating deep-seated tumors in 1982 using dynamic therapy. At present, it is the only place in the world where pion treatment is available.

In light of the small number of patients treated and the fact that only some of these were treated with dynamic therapy, it is not surprising that the clinical usefulness of pion therapy has not been established definitively. Some evidence indicates that pion therapy may be better than photon therapy for advanced prostate cancer (115) and inoperable soft- tissue sarcoma (116). However, pions have not demonstrated an advantage over fast neutrons for these two types of cancer. Intuitively, pions should be superior to neutrons

due to their Bragg peak. The fact that this superiority has not been observed suggests that, as is the case for neon ions, it is the high-LET character of the pion beam rather than the Bragg peak that produces favorable results. Further studies on dosimetry and the effects of dose fractionation nevertheless could lead to improved results with pions.

NEUTRON-CAPTURE THERAPY

Despite the best efforts of many researchers, some forms of cancer remain resistant to any form of therapy. These include melanoma and advanced brain tumors (in particular glioma). The main reason for the ineffectiveness of radiation therapy for glioma is that, in addition to the gross tumor visible on CT or MRI images, small clusters of unseen tumor cells are embedded in the healthy brain tissue. If the treatment volume includes this microscopic disease, too much healthy tissue is irradiated, and the patient experiences unacceptable brain damage. However, if the treatment volume is limited to the visible tumor, the disease recurs and ultimately causes death. In neutron-capture therapy, tumor cells are sensitized so that neutron irradiation of the brain selectively does more damage to these cancerous cells. The concept of using the high cross section for the production of alpha particles in interactions between thermal neutrons and ^{10}B to enhance the tumor dose was first suggested by Locher in 1936 (117). For glioma, it is possible to selectively introduce ^{10}B into the tumor by taking advantage of the blood-brain barrier, which protects healthy brain cells from toxins. Because the tumor is not protected by the blood-brain barrier, boron-containing drugs can be taken up by tumor cells yet be excluded from healthy cells. Similarly, to enhance tumor dose in melanoma, one can administer drugs which are absorbed preferentially by melanin.

Clinical Trials for Neutron-Capture Therapy

Clinical trials for glioma were conducted during the 1950s and early 1960s at Brookhaven National Laboratory (BNL) and the Massachusetts Institute of Technology (MIT). Results were unsatisfactory because of the poor penetrating ability of the thermal neutron beams and because the concentration of ^{10}B in the tumor was only marginally greater than that in the blood vessels. These investigations revealed that ^{10}B concentrations in the tumor must be significantly greater than both the healthy tissue concentration and the bloodstream concentration in order to deliver an acceptably low dose to healthy tissues. The MIT and BNL trials were stopped until more work, including biodistribution studies, could be done on drug development (118, 119). In Japan, Hiroshi Hatanaka has circumvented the problem of poor neutron penetration by treating residual glioma cells interoperatively during a surgical procedure to remove the gross tumor. Since 1968 he has treated more than 100 glioma patients using neutron beams from several reactors in Japan (120). During the surgery the patient is given an arterial infusion of sodium borocaptate (BSH) to sensitize the unresected tumor cells. Many of these patients have survived significantly longer than those treated with surgery and/or conventional radiation. At least three patients appear to have been cured (121, 122).

In 1987 Mishima et al began clinical trials for cutaneous melanoma using p-boronophenylalanine (BPA) with reactor-generated thermal neutrons. To date, at least six patients have been treated (123). BPA was chosen because it selectively delivers boron to the melanoma cells. This drug is also under investigation for its potential to deliver boron to gliomas and breast tumors (124). At present, the pharmacokinetics of both BSH and BPA are well enough understood to warrant further clinical trials for both glioma and melanoma. However, the lack of adequate neutron sources has slowed the ongoing work in Japan as well as the start of trials elsewhere.

Neutron Sources

Although thermal neutrons have optimal energies for interacting with ^{10}B in a tumor, they are not energetic enough to penetrate to the location of most tumors. An ideal clinical beam is thought to consist of epithermal neutrons that thermalize as they penetrate to the tumor. The energy range of 1 - 10 keV is expected to be optimal. Beams in this range have been extracted from nuclear reactors at BNL, MIT, the Georgia Institute of Technology Research, and the Joint Research Centre in Petten, The Netherlands (125-127). These groups anticipate clinical trials in the mid to late 1990s. Their beams are probably adequate for initial clinical trials, but many problems are associated with the use of nuclear reactors, not the least of which is the public's perception of them as being inherently unsafe. As has been true for the early work

with all forms of hadron therapy, a few beam lines originally built for basic physics research are undergoing remodeling to support clinical research. To acquire the statistics needed to demonstrate the efficacy of the therapy, neutron sources must be more easily available. An ideal source would be an accelerator similar in size to those presently used in hospitals.

Considerable study has been devoted to the use of a 2.5-MeV RFQ to produce neutrons via the $^{7}Li(p,n)^{7}Be$ reaction (128 - 130). A 2.5-MeV tandem cascade accelerator has also been designed to utilize this reaction (131). Both accelerators are similar in size to electron linacs used for conventional radiation therapy. However, neither has been developed to the point where it could be used for clinical trials, primarily because of the technical difficulties involved in cooling a lithium target. One can also use a beryllium target with a 4-MeV drift tube linac (132). Any of the schemes mentioned here requires a moderating system similar to those used with reactors. Their construction requires a significant research and development effort, which is hampered by lack of funding. An alternate neutron source is any high-current accelerator that delivers protons with energies of at least 70 MeV. In this case, the protons strike a heavy target to produce neutrons by spallation. The work on spallation sources at PSI is promising (133), but these sources are too large and expensive to be practical for most hospitals.

Alternate Approaches

The n + ^{157}Gd reaction can also be used for neutron-capture therapy. In this case, the dose is delivered by secondary gamma rays whose range is considerably longer than the range of alpha particles produced in the n+^{10}B reaction. This longer range is a disadvantage in terms of localizing the dose, but other features of the n+^{157}Gd reaction warrant its further investigation. In particular, the thermal neutron cross section for ^{157}Gd is ~64 times greater than for ^{10}B. ^{157}Gd is already in use as an enhancement material for MRI because it is a tumor seeking agent (134). In vitro and in vivo studies have also shown it to be useful in killing glioma cells (135). Further research is needed to establish whether the ^{10}B or ^{157}Gd reaction is optimal for neutron-capture therapy.

Another approach is the use of fast-neutron beams rather than epithermal beams. Clinical fast-neutron beams have energy spectra that include an epithermal component. Experience with fast-neutron therapy for glioma has shown that these beams do indeed kill the tumor cells without the addition of a dose-enhancing drug. However, a therapeutic window for a long-term cure has not been established (136), i.e. if the dose is large enough to destroy the tumor, then the patient dies from late effects caused by unavoidable dose to healthy brain tissue. A tumor dose enhancement as small as 10-20% may be adequate to define a therapeutic window. Biophysical studies with cell cultures and rodent tumors in fast-neutron beams have shown dose enhancements when ^{10}B is present in the tumor cells (137, 138). Neutron-capture therapy with fast neutrons has the disadvantage of lower n+^{10}B or n + ^{157}Gd cross sections, but it has better beam collimation and could be implemented at several existing accelerator-based fast-neutron therapy clinics.

SUMMARY AND DISCUSSION

Hadrons have biological and/or physical characteristics that enable them to be used to treat malignant tumors and other lesions that either do not respond well to conventional photon radiotherapy or are located close to critical structures, which limits the dose that may be delivered safely. These cases constitute about 15% of those that would normally be treated with radiation. The high LET of neutrons, pions, and heavy-charged particles provides a biological advantage, whereas the Bragg peak of protons and heavier ions allows the dose distribution to be conformed closely to the tumor volume. Table 3 summarizes these properties for each type of therapy discussed in this review and estimates in 1992 dollars the cost of the accelerators needed to provide the radiation. The costs listed do not include buildings and other clinical equipment.

Low-LET charged particles, in particular protons and helium ions, have been proven to be effective in treating skull-base tumors, including clival chordoma and chondrosarcoma, meningioma, craniopharyngioma, and pituitary adenoma. These particles have also been used successfully to treat uveal melanoma, with local-control rates of 97% or better, and have played an important role in treating arteriovenous malformations, especially large, irregularly shaped AVMs which are difficult to treat with existing conformal photon techniques. Recent work in Japan (79) indicated that protons can be used to advantage to treat diseases in the thorax, abdomen, and pelvis including cancers of the lung, esophagus,

Table 3 Summary of External Beam Radiotherapy Options for Malignant Tumors

Particle	Tumor Characteristics	Energy Deposition	Bragg Peak	Radiation Source	Accelerator Cost [a]
Photons	Rapidly growing Oxygenated	Low LET	No	Cobalt Electron linac	$1-2 M
Electrons	Superficial	Low LET	No	Electron linac	$1-2 M
Protons	Early stage, near critical structures	Low LET	Yes	Synchrotron Cyclotron	$10-15 M
Fast Neutrons	Slow growing, Hypoxic	High LET	No	Proton linac Cyclotron	$8-10 M
Heavy Ions	Same as fast neutrons	High LET	Yes	Synchrotron	$40 M
Pions	Same as fast neutrons	High LET	Yes	Proton linac Cyclotron	$35-40M
Slow Neutrons	Glioblastoma Some melanomas	Very high LET using ^{10}B drugs	No	Proton linac Nuclear reactor	$1-2 M

[a] In 1992 dollars, not including facility costs.

liver, uterine cervix, and prostate. Preliminary results are interesting because they point toward proton therapy applications that have received only limited attention in the past.

High-LET radiation has proven effective in treating recurrent salivary gland tumors, locally advanced prostate tumors, and bone and soft-tissue sarcoma. Clinical results (i.e. local-control and survival rates for these tumors) are very similar for fast neutrons and high-LET charged particles. Given the dose-distribution superiority of heavy ions, it is somewhat surprising that the results for neon ions are not better than those for fast neutrons. However, success with high-LET radiation depends on many variables including fractionation, total treatment time, and absolute dose. Until clinical trials designed to optimize these variables are completed, one cannot fully assess the importance of high-LET charged-particle radiation in the treatment of radioresistant tumors.

To clearly establish the role of hadronic therapy in cancer treatment we must continue to develop each modality, carefully documenting and comparing results in terms of quality of life, long-term side effects, and long-term posttreatment survival. Research will likely continue for protons and fast neutrons because the cost for these modalities is comparable to that of more conventional cancer treatments such as surgery or chemotherapy. Pion therapy continues only in Canada, and neutron-capture therapy is available only in Japan. However, the latter may become available at a few reactors in The Netherlands and the US by the end of the 1990s. LBL no longer provides heavy-ion therapy, although clinical trials are expected to start in Japan and Germany by the end of the 1990s. The usefulness of these more expensive forms of therapy will be adequately evaluated only if governments or other funding sources are willing to provide the necessary support.

ACKNOWLEDGMENTS

We wish to thank Joseph Castro, Lionel Cohen, and Frank Hendrickson for helpful discussions and suggestions. This work was supported in part by the U.S. Department of Energy contract No. DE-AC02-76CH03000.

Literature Cited

1. Wilson, RR. *Radiology* 47:487-491 (1946)

2. Tobias CA, Anger HO, Lawrence JH. *Am. J. Roentgenol. Radiat. Ther. Nucl. Med.* 67:1-27 (1952)

3. Tobias CA, Van Dyke DC, Simpson ME, Anger HO, Huff RL, Koneff AH. *Am. J. Roentgenol. Radiat. Ther. Nucl. Med.* 72:1-21 (1954)

4. Goitein M, Sisterson JM. *Radiat. Res.* 74:217-230 (1978)

5. Goitein M. Med. Phys. 5:258-264 (1978).

6. Urie M, Goitein M, Holley WR, Chen GTY. *Phys. Med. Biol.* 31:1-15 (1986)

7. Petti, PL. *Med. Phys.* 19:137-149 (1992)

8. Johns HE, Cunningham, JR. *The Physics of Radiology*, p. 675. Springfield, Ill: Charles C. Thomas - Publisher. 796 pp. (1983)

9. Smathers JB, Otte VA, Almond PR. In *Particle Radiation Therapy*, ed. VP Smith, pp. 33-57. Philadelphia: American College of Radiology. 572 pp. (1976)

10. Fowler JF. *Nuclear Particles in Cancer Treatment*. p. 32. Bristol: Adam Hilger Ltd. 178 pp. (1981)

11. Fowler JF. See Ref. 10, p. 100 (1981)

12. Fowler JF. In *The Biological Basis for Radiotherapy*, eds. GG Steel, GE Adams, MJ. Peckham pp. 261-68. New York: Elsevier (1983)

13. Fowler JF. *Radiology* 108:139-43 (1972)

14. Stone RS, Lawrence JH, Aebersold PC. *Radiology* 35:322-27 (1940)

15. Stone RS. *Am. J. Roentgenology* 59:771-85 (1948)

16. Fowler JF, Morgan RL. *Brit. J. Radiol.* 36:115-21 (1963)

17. Bewley DK, Fowler JF, Morgan RL, et al. *Brit. J. Radiol.* 36:107-15 (1963)

18. Catterall M, Bewley D. *Fast Neutrons in the Treatment of Cancer,* p. 5. London: Academic Press. 394 pp. (1979)

19. Broerse JJ, Mijnheer BJ. In *Progress in Medical Radiation Physics,* ed. CG. Orton, p 3. New York: Plenum Press (1982)

20. Schreuder AN, Jones DTL, Symons JE, Fulcher T, Bredenkamp P, Kiefer A. In *Proc. Int. Symp. on Hadron Therapy, Como, Italy, Oct. 18-21, 1993,* ed U. Amaldi, B. Larsson, Oxford:Elsevier. In Press (1994)

21. Saroja KR, Mansell J, Hendrickson FR, Cohen L, Lennox A. *Int. J. Radiation Oncology Biol. Phys.* 13: 1319-25 (1987)

22. Laramore GE. *Int. J. Radiation Oncology Biol. Phys.* 13: 1421-23 (1987)

23. Laramore GE, Krall JM, Thomas FJ, Russell KJ, Maor MH, et al. *Am. J. Clin. Oncol. (CCT)* 16(2):164-67 (1993)

24. Griffin TW, Krall JM, Laramore GE, Parker RG, Burnison M, et al. *Int. J. Radiation Oncology Biol. Phys.* 27/S1:247 (1993)

25. Koh WJ, Krall JM,.Peters LJ,.Maor MH, Laramore GE, et al. *Int. J. Radiation Oncology Biol. Phys.* 27:499-505 (1993)

26. Laramore GE, Griffith JT, Boespflug M, Pelton JG, Griffin T, et al. *Am J Clin Oncol(CCT)* 12(4):320-26 (1989)

27. Saroja KR, Mansell J, Hendrickson FR, Cohen L, Lennox A. *Int. J. Radiation Oncology Biol. Phys.* 17: 1295-97 (1989)

28. Lennox AJ. *Nucl. Instr. and Meth. B* 56/57:1197-1200 (1991)

29. Janni JF. *Calculations of energy loss, range, pathlength, straggling, multiple scattering, and the probability of inelastic nuclear collisions for 0.1- to 1000-MeV protons.* Reproduced by the National Technical Information Service, U.S. department of Commerce, Springfield, VA 22151, AFWL-TR-65-150 (1966)

30. Chen GTY, Singh RP, Castro JR, Lyman JT, Quivey JM. *Int. J. Radiat. Oncol. Biol. Phys.* 5:1809-19 (1979)

31. Kijewski PK, Bjärngard BE. *Int. J. Radiat. Oncol. Biol. Phys.* 4:429-35 (1978)

32. Alpen EL, Saunders W, Chatterjee A, Llacer J, Chen GTY, Scherer J. *Brit. J. Radiol.* 58:542-48 (1985)

33. Goitein M. *Int. J. Rad. Onc. Biol. Phys.* 4:499-508 (1978)

34. Urie M, Goitein M, Wagner M. *Phys. Med. Biol.* 29:553-566 (1983)

35. Koehler AM. In: *Proc. Symposium on Pion and Proton Radiography,* pp. 63-68. National Accelerator Laboratory, Batavia, Illinois (1971)

36. Chu WT, Ludewigt BA, Renner TR. *Rev. Sci. Instrum.* 64(8):2055-2122 (1993)

37. Wilson RR. *Phys. Rev.* 71:385-86 (1947)

38. Koehler AM, Schneider RJ, Sisterson JM. *Nucl. Instrum. Meth.* 131:437-40 (1975)

39. Koehler AM, Preston,WM. *Radiology* 104:191-95 (1972)

40. Coutrakon G, Bauman M, Lesyna D, Miller D, Nusbaum J, et al. *Med. Phys.* 18:1093-99 (1991)

41. Lyman JT. In *Pion and Heavy Ion Radiotherapy: Pre-Clinical and Clinical Studies,* ed. LD Skarsgard, p 139. New York: Elsevier (1983)

42. Petti PL, Lyman JT, Renner TR, Castro JR, Collier JM, et al. *Med. Phys.* 18:513-18 (1991)

43. Ludewigt BA, Chu WT, Phillips MH, Renner TR. *Med.Phys.* 18:36-42 (1991)

44. van den Elsen PA, Pol EJD, Viergever MA. *IEEE Engineering in Med. and Biol.* 12:26-39 (1993).

45. Kessler ML, Pitluck S, Petti PL, Castro JR. *Int. J. Radiat. Oncol. Biol. Phys.* 21:1653-1667 (1991).

46. Fraass BA, McShan DL, Diaz RF, Ten Haken RK, Aisen A, et al. *Int. J. Radiat. Oncol. Biol. Phys.* 13:1897-1908 (1987).

47. Pelizzari C, Chen GTY. *J. Computer Aided Tomography* 13:20 (1989).

48. Petti PL, Kessler ML, Fleming T, Pitluck S. Med. Phys. (accepted) (1994).

49. Goitein M, Abrams M, Rowell D, Pollari H, Wiles J. *Int. J. Radiat. Oncol. Biol. Phys.* 9:789-97 (1983)

50. Castro JR, Collier JM, Petti PL, Nowakowski V, Chen GTY, et al. *Int . J. Radiat. Oncol. Biol. Phys.* 17:477-84 (1989)

51. *Particles: A newsletter for those interested in proton, light ion and heavy charged particle radiotherapy.* ed. J. Sisterson. Cambridge (1993)

52. Saunders WM, Chen GTY, Austin-Seymour M, Castro JR, Collier JM, et al. *Int. J. Radiat. Oncol. Biol. Phys.* 11:1339-47 (1985)

53. Austin-Seymour M, Munzenrider JE, Goitein M, Verhey L, Urie M, et al. *J. Neurosurg.* 70:13-17 (1989)

54. Castro JR, Linstadt DE, Bahary JP, Petti PL, Daftari, et al. *Int. J. Radiat. Oncol. Biol. Phys.* In press (1994)

55. Berson AM, Castro JR, Petti PL, Phillips TL, Gauger GE, et al. *Int. J. Radiat. Oncol. Biol. Phys.* 15:559-65 (1988)

56. Char DH, Castro JR, Quivey JM, Phillips TL, Irvine AR, et al. *Ophthalmology* 96:1708-15 (1989)

57. Char DH, Castro JR. In *Recent Advances in Ophthalmology* ed. SI Davidson, B Jay, pp. 169-83. New York: Churchill Livingstone (1992)

58. Stallard HB. *Mod. Probl. Ophthalmol.* 7:16-38 (1968)

59. MacFaul PA. *Trans.Ophthalmol. Soc. UK* 97:421-27 (1977)

60. Lommatzsch PK. *Arch. Ophthalmol.* 101:713-17 (1983)

61. Busse H, Muller RP, Kroll P. *Am. J. Ophthalmol.* 15:1146-49 (1983)

62. Gass JD. *Arch.Ophthalmol.* 103:916 (1985)

63. Bosworth JL, Packer S, Rotman M, et al. *Radiology* 169:249 (1988)

64. Munzenrider JE, Verhey L, Gragoudas ES, Seddon JM, Urie M, et al. *Int. J. Radiat. Oncol. Biol. Phys.* 17:493-98 (1989)

65. Linstadt DE, Castro JR, Char DH, Decker M, Ahn D, et al. *Int. J. Radiat. Oncol. Biol. Phys.* 19:613-18 (1990)

66. Char DH, Castro JR, Kroll SM, Irvine AR, Quivey JM, Stone RD. *Arch. Ophthalmol.* 108:209-14 (1990)

67. Munzenrider JE, Gragoudas ES, Seddon JM, Sisterson J, McNulty P, et al. *Int. J. Radiat. Oncol. Biol. Phys.* 15:553-58 (1988)

68. Egan K, Gragoudas ES, Seddon JM, Glynn RJ, Munzenrider JE, et al. *Ophthalmol.* 96:1377-83 (1989)

69. Fabrikant JI, Levy RP, Steinberg GK, Phillips MH, Frankel KA, et al. *Sterotactic Radiosurgery* 3:99-139 (1992)

70. Kjellberg RN, Poletti CE, Roberson GH, et al. In *Neurological Surgery with Emphasis on Non-Invasive Methods of Diagnosis and Treatment*, ed. R. Carrea, D. LeVay, pp. 181-87. Amsterdam: Excerpta Medica (1978)

71. Kjellberg RN, Hanamura T, Davis KR, et al. *N. Engl. J. Med.* 309:269-74 (1983)

72. Kjellberg RN, Davis KR, Lyons SL, et al. *Clin. Neurosurg.* 31:284-90 (1984)

73. Kjellberg RN. *Ann. Clin. Res.* 18 (Suppl. 47):17-19 (1986)

74. Kjellberg RN. In *Operative Neurosurgical Techniques*, (vol. 1). ed. HH Schmidek, WH Sweet, pp. 911-15. New York: Grune & Stratton (1988)

75. Kjellberg RN, Candia GJ. In *Harvard Radiosurgery Update*, Harvard Medical School, Chestnut Hill, MA (Abstr.) (1990)

76. Crawford PM, West CR, Chadwick DW, et al. *J. Neurol. Neurosurg. Psychiatry* 49:1-10 (1986)

77. Minakova YeI. In *Proc. 2nd. Int. Charged Particle Workshop, Loma Linda*, pp. 1-23 (1987)

78. Minakova YeI. In *Proc. Int. Heavy Particle Therapy Workshop, Paul Scherrer Institute, Sept 1989.* ed. H. Blattmann, Villigen, Switzerland PSI-Bericht 69:158-62 (1990)

79. Minokova YeI, Krymsky VA, Luchin YeI, et al. *Med. Radiol. (Mosk.)* 32:36-42 (1987)

80. Alexander E, Loeffler JS, Lunsford LD. *Stereotactic Radiosurgery*, New York: McGraw-Hill, Inc. 254 pp. (1993)

81. Saunders W, Castro JR, Chen GTY, Collier JM, Zink SR, et al. *Radiat. Res.* 104:S227-34 (1985)

82. Castro JR, Saunders WM, Chen GTY, Collier JM, Pitluck S, et al. *Am J. Clin Oncol.* 6:629-37 (1983)

83. Tsujii H, Tsuji H, Inada T, Maruhashi A, Hayakawa Y. et al. *Int. J. Radiat. Oncol. Biol. Phys.* 25:49-60 (1993)

84. Chu WT, Staples JW, Ludewigt BA, Renner TR, Singh RP, et al. *LBL Tech. Rep. LBL-33749*, Lawrence Berkeley Laboratory, Berkeley, California (1993)

85. Bloch C, Derenchuk V, Cameron J, Fasano M, Gilmore J, Hashemian R. *Nucl. Instrum. Methods in Phys. Res.* B79:890-94 (1993)

86. Pedroni E, Bacher R, Blattmann H, Boehringer T, Coray A, et al. See Ref.78, pp. 1-8 (1990)

87. Jones DTL, Yudelev M. See Ref. 78, pp. 77-81 (1990)

88. Fukumoto S, Endo K, Muto M, Akisada T, Kitagawa T, et al. See Ref. 78 pp. 70-74 (1990)

89. Fukumoto S. In *Proc. NIRS Int. Workshop on Heavy Charged Particle Therapy and Related Subjects, Chiba Japan, July 1991*, ed. A Itano, T Kanai, pp. 6-12. Chiba, Japan (1991)

90. Kawachi K. In *Proc. Fifth PTCOG Meeting and Int. Workshop on Biomedical Accelerators, Lawrence Berkeley Laboratory, December 1-2, 1986*, ed. WT Chu, LBL-22962:73-91. Berkeley California (1987)

91. Khoroshkov VS, Onosovsky KK, Breev VM, Goldin LL, Kleinbock MF, et al. See Ref. 90, pp. 204-212 (1991)

92. Khoroshkov VS, Goldin L, Onosovsky K, Klenov G. *Moscow Proton Therapy Facility Project*, Presented at 13th PTCOG Meeting, November 1990, Lawrence Berkeley Laboratory, Univ. of Calif., Berkeley, California (unpublished) (1990)

93. Linz U, Maier R. In *Proc. 1992 European Part. Accel. Conf. (EPAC).* In press (1994)

94. Cera, F, Cherubini R, Haque AMI, :Moschini G, Tiveron P, et al. *Radiological Research with Charged Particles at the Laboratori Naxionali di Legnaro (LNL).* Presented at the Fourth Workshop on Heavy Charged Particles in Biology and Medicine and XV PTCOG Meeting, Gesellschaft für Schwerionenforschung (GSI), September 23-25, 1991. Darmstadt, Extended Abstract, Report GSI-91-29, ISSN 0171-4546, paper K2 (1991)

95. Goodman, G. Presented at the International Heavy Particle Therapy Workshop, Paul Scherrer Institute, Villigen, Switzerland (1989)

96. Amaldi U, Silari M. *The TERA Project and the Centre for Oncological Hadrontherapy*, Rome:Istituto Nazionale Di Fisica Nucleare. 557 pp. (1994)

97. Martin RL. *Nucl. Instrum. Methods in Phys. Res.* B40/41:1331-34 (1989)

98. Hamm RW, Crandall KR, Potter JM, In *Proc. 1991 Part. Accel. Conf.*, IEEE #91CH3038-7:2583-85 (1991)

99. Scharf WH. *Biomedical Particle Accelerators*, Woodbury, NY:AIP Press. 731 pp. (1994)

100. Chadwick KH, Leenhouts HP.*Phys. Med. Biol.* 18:78-87 (1973)

101. Kellerer AM, Rossi HH. *Curriculum Topics Radiat. Res.* 8:85 (1972)

102. Kellerer AM, Rossi HH.*Radiat. Res.* 75:471-88 (1978)

103. Douglas BG, Fowler JF. *Radiat. Res.* 66:401-26 (1976)

104. Linstadt DE, Castro JR, Phillips TL. *Int. J. Radiat. Onc. Biol. Phys.* 20:761-69 (1991)

105. Batterman JJ, Breur K, Hart GAM, Van Peperzeel HA. *Eur. J. Cancer Clin. Oncol.* 17:539-48 (1981)

106. Batterman JJ, *Clinical application of fast neutrons: the Amsterdam experience* p. 114, Doctoral Thesis, University of Amsterdam 124 pp. (1981)

107. Schoenthaler R, Castro JR, Halberg FE, Phillips TL. *Int. J. Radiat. Onc. Biol. Phys.* 27:75-82 (1993)

108. Kraft G. See Ref. 20 (1994)

109. Sato K, et al. *Part. Accel.* 33:147-52 (1990)

110. Regler M. See Ref. 20 (1994)

111. Raju M. *Heavy Particle Radiotherapy*, pp. 356-450. New York: Academic Press 500 pp. (1980)

112. Curtis SB, Raju MR. *Radiat. Res.* 34:239-55 (1968)

113. Blattmann H. In *Boron Neutron Capture Therapy*, ed. D.Gabel and R. Moss. pp. 129-141. New York: Plenum Press (1992)

114. Boyd D, Schwettman HA, Simpson JA. *Nucl. Instrum. Meth.* 11: 315-31(1973)

115. Pickles T, Bowen J, Dixon P, Gaffney C, Pomeroy M, et al. *Int.J. Radiation Oncology Biol. Phys.*, 21:1005-11 (1991)

116. Greiner RH, Blattmann HJ, Thum P, Coray A, Crawford J, et al. *Int. J. Radiation Oncology Biol. Phys.* 17:1077-83 (1989)

117. Locher GL. *Am. J. Roentgenol.* 36:1-13 (1936)

118. Slatkin, DN. *Brain* 114:1609-29 (1991)

119. Asbury AK, Ojeann RG, Nielsen SL, Sweet WH. *J. Neuropathol Exp Neurol* . 31:278-303 (1972)

120. Hatanaka H, Amano K, Kamano S, Sano K. In *Neutron Capture Therapy - Proc. 2nd Int. Symposium on Neutron Capture Therapy,* ed. H Hatanaka, pp. 447-49. Norwell, Massachusetts: MTP Press. 449 pp. (1986)

121. Hatanaka H, Kamano S, Amano K, Hojo S, Sano K, et al. In *Boron neutron capture therapy for tumors*, ed. H Hatanaka, pp. 349-78. Niigata, Japan: Nishimura Co., Ltd.(1986)

122. Hatanaka H, Sano K, Yasukochi H. In *Progress in Neutron Capture Therapy for Cancer,* eds. B Allen, D Moore, B Harrington, pp. 551-56. New York: Plenum Press. 668 pp. (1992)

123. Mishima Y, Ichihashi M, Honda C, Shiono M, Nakagawa T, Obara H. See Ref. 122, pp. 577-83 (1992)

124. Coderre JA. See Ref. 113, pp. 111-21 (1992)

125. Fairchild RG, Benary V, Kalef-Ezra J, Saraf SK, Brugger RM, et al. See Ref. 122, pp. 1-6 (1992)

126. Moss RL, Stecher-Rasmussen F, Huiskamp R, Dewit L, Mijnheer B. See Ref. 122, pp. 7-12 (1992)

127. Zamenhof R, Madoc-Jones H, Harling O, Wazer D, Saris S, et al. See Ref. 122, pp. 21-26 (1992)

128. Lone MA, Ross AM, Fraser JS, Schriber SO, Kushneriuk SA, Selander WN. *Low Energy 7Li(p,n)7Be Neutron Source (Canutron).* Chalk River Laboratories, Internal Report AECL-7413 (1982)

129. Blue JW, Roberts WK, Blue TE, Gahbauer RA, Vincent JS. See Ref. 120, pp. 147-58 (1986)

130. Wangler TP, Stovall JE, Bhatia TS, Wang CK, Blue TE, Gahbauer RA. In *Proc. 1989 IEEE Part. Accel. Conf.*, IEEE #89CH2669-0, pp. 678-80 (1989)

131. Shefer RE, Klinkowstein RE, Yanch JC, Brownell GL. See Ref. 122, pp. 119-22 (1992)

132. Wang C-KC, Moore BR. In *Advances in Neutron Capture Therapy,* eds. AH Soloway, RF Barth, DE Carpenter, pp.125-129. New York:Plenum Press. 829 pp. (1993)

133. Crawford JF, Reist H, Conde H, Elmgren K, Roennqvist T, et al. See Ref. 122, pp. 129-32 (1992)

134. Oda Y, Takagaki M, Miyatake S, Kikuchi H. *Neurosurgery Letters* 1(5):11-16 (1991)

135. Takagaki M, Oda Y, Miyatake S, Kikuchi H, Kobayashi T, et al. See Ref. 122, pp. 407-10 (1992)

136. Saroja KR, Mansell J, Hendrickson FR, Cohen L, Lennox A. *Int. J. Radiat. Oncology Biol. Phys.* 17:1295-97 (1989)

137. Sauerwein W. Presented at Int. Symp. Neutron Capture Therapy, 5th, Columbus (1992).

138. Wooton P, Risler R, Livesey J, Brossard S, Laramore G, Griffin T. See Ref. 122, pp. 195-98 (1992)